Evolutionary Dynamics of Floral Homeotic Transcription Factor Protein–Protein Interactions

Madelaine Bartlett,*[,1,2] Beth Thompson,[3] Holly Brabazon,[2] Robert Del Gizzi,[1] Thompson Zhang,[1] and Clinton Whipple*[,2]

[1]Department of Biology, University of Massachusetts Amherst

[2]Department of Biology, Brigham Young University

[3]Department of Biology, East Carolina University

***Corresponding author:** E-mail: mbartlett@bio.umass.edu; whipple@byu.edu.

Associate editor: Gunter Wagner

Abstract

Protein–protein interactions (PPIs) have widely acknowledged roles in the regulation of development, but few studies have addressed the timing and mechanism of shifting PPIs over evolutionary history. The B-class MADS-box transcription factors, PISTILLATA (PI) and APETALA3 (AP3) are key regulators of floral development. PI-like (PI^L) and AP3-like ($AP3^L$) proteins from a number of plants, including *Arabidopsis thaliana* (Arabidopsis) and the grass *Zea mays* (maize), bind DNA as obligate heterodimers. However, a PI^L protein from the grass relative *Joinvillea* can bind DNA as a homodimer. To ascertain whether *Joinvillea* PI^L homodimerization is an anomaly or indicative of broader trends, we characterized PI^L dimerization across the Poales and uncovered unexpected evolutionary lability. Both obligate B-class heterodimerization and PI^L homodimerization have evolved multiple times in the order, by distinct molecular mechanisms. For example, obligate B-class heterodimerization in maize evolved very recently from PI^L homodimerization. A single amino acid change, fixed during domestication, is sufficient to toggle one maize PI^L protein between homodimerization and obligate heterodimerization. We detected a signature of positive selection acting on residues preferentially clustered in predicted sites of contact between MADS-box monomers and dimers, and in motifs that mediate MADS PPI specificity in Arabidopsis. Changing one positively selected residue can alter PI^L dimerization activity. Furthermore, ectopic expression of a *Joinvillea* PI^L homodimer in Arabidopsis can homeotically transform sepals into petals. Our results provide a window into the evolutionary remodeling of PPIs, and show that novel interactions have the potential to alter plant form in a context-dependent manner.

Key words: **PISTILLATA, Poales, APETALA3, convergent molecular evolution, B-class MADS box genes, evolution of flower development.**

Article

Introduction

Gene regulation during development involves a complex interplay between DNA, RNA, and protein, resulting ultimately in organismal phenotype. Altered gene regulation, over the course of evolution, is one important mechanism through which phenotypes change. Regulatory landscapes evolve because of both noncoding and coding changes in the genome. Although noncoding changes play important roles in the evolution of organismal form (Stern 2000; Wray et al. 2003; Carroll 2005; Wittkopp and Kalay 2012; Della Pina et al. 2014), coding changes can also effect phenotypic change (Stern and Orgogozo 2008; Bartlett and Whipple 2013). Altered protein–protein interactions (PPIs), particularly between transcription factors, represent an example of coding change that can alter phenotype (Löhr and Pick 2005; Veron et al. 2007; Lynch and Wagner 2008; Airoldi et al. 2010; Brayer et al. 2011; Baker et al. 2012). Although we have learned much about how PPIs can alter transcription factor function (Adhikary and Eilers 2005; Slattery et al. 2011; Kong et al. 2012; Sayou et al. 2014), few studies have addressed the precise course and potential of PPI evolution (but see Yasumura et al. 2007; Melzer et al. 2014). To understand how novel transcription factor PPIs arise, and how they change over time, PPIs need to be investigated in an explicitly evolutionary context.

One transcription factor family that has been extensively investigated in plants is the MIKC MADS-box transcription factors. MADS-box transcription factors are present in all eukaryotic lineages and named for the first cloned representatives: MEF2, AGAMOUS, DEFICIENS, and SRF. The plant-specific MIKC MADS-box proteins have a characteristic domain structure: A DNA-binding MADS-box, intervening loop domain, keratin-like coiled-coil domain, and a disordered C-terminus (reviewed in Immink et al. 2010). MIKC MADS-box proteins are important regulators of floral development. In the ABC(E) model of floral development, floral organ identity is determined by the combinatorial action of ABC(E) MADS-box genes. For example, B-, C- and E-class functions together confer stamen identity, whereas C- and E-class functions together confer carpel identity (Coen and Meyerowitz

1991; Pelaz et al. 2000; Honma and Goto 2001). The ABC(E) model was originally derived using genetic mutants of Arabidopsis and *Antirrhinum majus* (snapdragon), but some of its core components, particularly B- and C-class functions, are broadly conserved in the angiosperms (reviewed in Litt and Kramer 2010; Smaczniak, Immink, Angenent, et al. 2012; Ó'Maoiléidigh et al. 2014).

Interactions between floral MADS-box proteins are critical for function. MADS-box proteins only bind DNA as dimers (Pellegrini et al. 1995) and the "floral quartet" model predicts that floral MADS-box proteins function as tetramers in planta (Theissen and Saedler 2001). A growing body of evidence supports the floral quartet model, and shows that higher-order PPIs are fundamental to floral MADS-box protein function (Honma and Goto 2001; Kaufmann et al. 2009; Smaczniak, Immink, Muino, et al. 2012; Mendes et al. 2013; Puranik et al. 2014). Interactions between MADS-box transcription factors can also have more subtle roles in the regulation of target genes. For example, E-class SEPALLATA (SEP) proteins of Arabidopsis bind DNA cooperatively. Thus, MADS-box PPIs have the capacity to influence the kinetics of DNA-binding, which may, in turn, affect downstream gene regulation and functional diversification (Jetha et al. 2014).

Changes to MADS-box PPIs have been implicated in phenotypic change. In *Eschscholzia californica* and *Thalictrum thalictroides*, mutations that disrupt MADS-box PPIs result in altered floral morphologies (Galimba et al. 2012; Lange et al. 2013). In snapdragon, shifting PPIs contributed to subfunctionalization of the C-class proteins PLENA and FARINELLI (Airoldi et al. 2010). In the oil palm, *Elaies guineensis*, two independent mutations that affect MADS-box dimerization underlie a modified fruit morphology that has been a target of selection in breeding (Singh et al. 2013). In the genus *Medicago*, the evolution of coiled fruit form is associated with stronger MADS-box PPIs (Fourquin et al. 2013). The evolution of B-class MADS-box PPIs, in particular, correlates with the evolution of some floral traits (Hernandez-Hernandez et al. 2007; Theissen and Melzer 2007; Lenser et al. 2009; Liu et al. 2010; Melzer et al. 2014). Floral development is more canalized in the eudicots and in many monocots, and B-class dimerization patterns have been connected to this canalization, particularly in the lineage leading to the core eudicots (Winter et al. 2002; Lenser et al. 2009; Melzer et al. 2014).

The B-class proteins APETALA3 (AP3) and PISTILLATA (PI) control petal and stamen development and are encoded by genes that are the product of a gene duplication event that predates angiosperm diversification (Kim et al. 2004). B-class function appears to be deeply conserved. In monocots and eudicots, B-class mutants exhibit similar phenotypes in which second whorl (petal) and third whorl (stamen) development is disrupted (Ambrose et al. 2000; Nagasawa et al. 2003; Vandenbussche et al. 2004; Drea et al. 2007; Kramer et al. 2007; Roque et al. 2013; Sharma and Kramer 2013; Quinet et al. 2014; Zhang et al. 2014; Bartlett et al. 2015). Despite a high degree of sequence similarity and overlapping expression domains, $AP3^L$ and PI^L proteins are broadly nonredundant (Jack et al. 1992; Goto and Meyerowitz 1994; Ambrose et al. 2000; Bartlett et al. 2015). This nonredundancy is due in part to their PPI landscape: In many lineages, $AP3^L$ and PI^L proteins bind DNA as obligate heterodimers (summarized in Melzer et al. 2014). $AP3^L/PI^L$ heterodimers in Arabidopsis, maize, and snapdragon also regulate their own expression through autoregulatory feedback loops (Schwarz-Sommer et al. 1992; Goto and Meyerowitz 1994; Jack et al. 1994; Riechmann, Krizek, et al. 1996; Bartlett et al. 2015).

Broad surveys of B-class dimerization across the angiosperms show that although obligate $PI^L/AP3^L$ heterodimerization is pervasive in the eudicots, both PI^L and $AP3^L$ homodimerization occur across the tree, particularly in monocots and in early-diverging angiosperms (Winter et al. 2002; Melzer et al. 2014). For example, PI^L proteins homodimerize in both *Amborella trichopoda* and the magnoliid *Liriodendron tulipfera* (Melzer et al. 2014). In the monocots, PI^L proteins from *Lilium* (Winter et al. 2002; Chen et al. 2011), *Tulipa* (Kanno et al. 2003), and the orchid *Phalaenopsis equestris* (Tsai et al. 2008) both homo- and heterodimerize with $AP3^L$ proteins (facultative homodimerization). The single identified PI^L protein from the close grass relative *Joinvillea* (J-PI) also homodimerizes (Whipple and Schmidt 2006). Ancestral state reconstructions integrating all available interaction data indicate that $AP3^L/PI^L$ heterodimerization evolved early on in angiosperm history from facultative $AP3^L$ and/or PI^L homodimerization (Winter et al. 2002; Melzer et al. 2014). How variable B-class dimerization is on smaller evolutionary timescales (within individual families and orders) is still unclear.

Here, we report on the evolution of B-class dimerization in the Poales, and on our molecular characterization of obligate heterodimerization versus homodimerization in the order. Our survey of B-class dimerization revealed an unexpected level of evolutionary change. Our analyses indicate multiple transitions between facultative PI^L homodimerization and obligate $PI^L/AP3^L$ heterodimerization in the Poales. Ancestral state reconstructions and population genetic data show that the obligate heterodimerization characteristic of one maize B-class protein STERILE TASSEL SILKY EAR1 (STS1) is a derived state, evolved recently from PI^L homodimerization, and fixed during maize domestication. Although STS1 forms obligate heterodimers with the single maize AP3 homolog SILKY1 (SI1), its ortholog in *Brachypodium distachyon* (BdSTS1) can homodimerize, as can the *Joinvillea* PI^L protein J-PI (Whipple and Schmidt 2006; Bartlett et al. 2015). Thus, comparisons between BdSTS1, J-PI, and STS1 provide a framework to investigate the molecular underpinnings of B-class homo- versus heterodimerization. We identified domains and residues that mediate homo- versus heterodimerization of PI^L proteins in the Poales. Finally, we show that altered B-class PPIs can affect phenotype in a heterologous system.

Results

PI^L Dimerization Patterns Are Labile in the Poales

Cases of PI^L homodimerization have been reported in the monocots (most recently summarized in Melzer et al. 2014), but it was not clear whether these represented isolated curiosities or were indicative of broader evolutionary trends.

To address this question, we used gel shift assays to survey 31 PI^L proteins from 18 taxa spanning the Poales. We incubated a labeled DNA probe containing a known PI/AP3 binding site (Riechmann, Krizek, et al. 1996; Riechmann, Wang, et al. 1996; Hill et al. 1998) and one or more B-class proteins. Given that MADS-box proteins bind DNA as dimers, if we observed a shift when a single protein was added, we concluded the protein could bind DNA as a homodimer. Our analyses represent the first biochemical assays for most proteins under investigation. We found incidences of obligate $AP3^L/PI^L$ heterodimerization, PI^L homodimerization, and of $AP3^L$ homodimerization (fig. 1A–*D*, complete results in supplementary fig. S1, Supplementary Material online). A SI1 C-terminal truncation (SI1-C) formed artifactual homodimers in gel shift assays (fig. 1A and supplementary fig. S1, Supplementary Material online). Our results were consistent with published work, except for a single report on *Oryza sativa* PI-1 (OsMADS4) (Ronai et al. 2003). OsMADS4 did not form homodimers in yeast two-hybrid assays (Moon et al. 1999), and did not form homodimers in our gel shift assays (supplementary fig. S1, Supplementary Material online). Thus, we scored OsMADS4 as an obligate heterodimer. A second anomaly involved B-class proteins from the grass *Pharus virescens*. Although neither *Pharus* PI-1 nor *Pharus* PI-2 formed detectable homodimers in our gel shifts, we did not detect reliable interactions with any $AP3^L$ protein. Therefore, we scored both *Pharus* PI-1 and PI-2 as equivocal in all downstream analyses.

Select interactions were further examined using bimolecular fluorescence complementation (BiFC) and yeast two-hybrid assays (fig. 1E–*K* and supplementary fig. S2, Supplementary Material online). The yeast two-hybrid assays produced spurious interactions when both tested proteins were truncated (IKC constructs) (similar results in Leseberg et al. 2008), and full-length proteins did not interact in yeast (even at 22 °C), as reported for other B-class proteins (data not shown, Honma and Goto 2001; Yang, Fanning, et al. 2003; de Folter et al. 2005). Therefore, we tested interactions using a full-length protein fused to the DNA-binding domain and a truncated IKC protein fused to the activation domain. All BiFC assays were performed with full-length protein in both directions. All three assays produced similar results, although with some minor inconsistencies (fig. 1 and supplementary fig. S1, Supplementary Material online). We used gel shifts to further investigate B-class PPIs because we could consistently use full-length proteins and assay DNA-binding as a consequence of dimerization. As B-class proteins are DNA-binding transcription factors, electrophoretic mobility shift assays (EMSAs) provided the most robust and biologically relevant assay.

PI^L dimerization patterns are unexpectedly labile across the Poales. We mapped known PI^L EMSA dimerization states onto a Bayesian gene phylogeny, including interactions described here (fig. 1L and supplementary fig. S3, Supplementary Material online). Although many more monocot PI^L sequences are available, we included only those assayed for dimerization. We reconstructed ancestral dimerization states using maximum-likelihood and parsimony methods, as implemented in Mesquite V2.75 (Maddison and Maddison 2009). The parsimony reconstructions also used synthetic species trees that reflect current best estimates of relationships in the order (Givnish et al. 2010; GPWG II 2012; Bouchenak-Khelladi et al. 2014). The state at the base of the Poales was reconstructed as more likely to be homodimerizing, with or without non-Poalean outgroups (node 1, fig. 1 and supplementary fig. S4, Supplementary Material online). Similarly, the most parsimonious state at the base of the Poales is reconstructed as either equivocal or PI^L homodimerization (supplementary fig. S4, Supplementary Material online). These results suggest that the *Joinvillea* PI^L protein has retained the ability to homodimerize (Whipple and Schmidt 2006) from an ancestral condition in the Poales. We cannot precisely reconstruct the ancestral state at the base of the Poales, or the precise history of changes in B-class dimerization. However, both PI^L homodimerization and obligate heterodimerization occur, and B-class interactions have clearly been in flux across the order.

Obligate Heterodimerization and PI^L Homodimerization Evolved Convergently in the Grasses

PI^L dimerization has also been in flux within the grass family. Obligate heterodimerization is the more likely ancestral state at the base of the grasses (node 2, fig. 1L and supplementary fig. S4, Supplementary Material online), but homodimerization has emerged within the family. Within the grasses, *PI^L* genes have duplicated, resulting in two gene clades, *PI-1* and *PI-2* (Munster et al. 2001; Whipple et al. 2007). PI-1 proteins have retained the most likely ancestral condition of obligate heterodimerization. In contrast, PI^L homodimerization emerged within the PI-2 clade, prior to the diversification of the hyperdiverse BEP and PACMAD clades (fig. 1L, node 6). Although we cannot pinpoint exactly when PI^L homodimerization emerged in the grass PI-2 gene clade, ancestral state reconstructions suggest that J-PI homodimerization and the homodimerization characteristic of many grass PI-2 proteins are most likely independently derived. Our analyses unequivocally reconstruct obligate heterodimerization between the maize PI-2 protein, STS1, and the AP3 ortholog SI1 as a derived character state, evolved from PI^L homodimerization. Thus, the obligate heterodimerization characteristic of the PI-1 and PI-2 proteins of maize (Whipple et al. 2007; Bartlett et al. 2015) has arisen independently.

If PI^L homodimerization and obligate heterodimerization did arise de novo in the grass PI-2 gene lineage, and if there is more than one path to each dimerization state, the molecular determinants of obligate heterodimerization versus homodimerization would likely be distinct between J-PI, PI-2 from *B. distachyon* (BdSTS1), and PI-2 from maize (STS1). In order to identify which protein domains were determining obligate heterodimerization versus homodimerization in the Poales, we performed domain swap experiments. Because the I and K domains are critical for the AP3/PI interaction in Arabidopsis (Riechmann, Krizek, et al. 1996; Krizek and Meyerowitz 1996b; Yang, Fanning, et al. 2003; Yang, Xiang, et al. 2003; Yang and Jack 2004), we first swapped the I and K domains between BdSTS1 and STS1, and between J-PI and STS1.

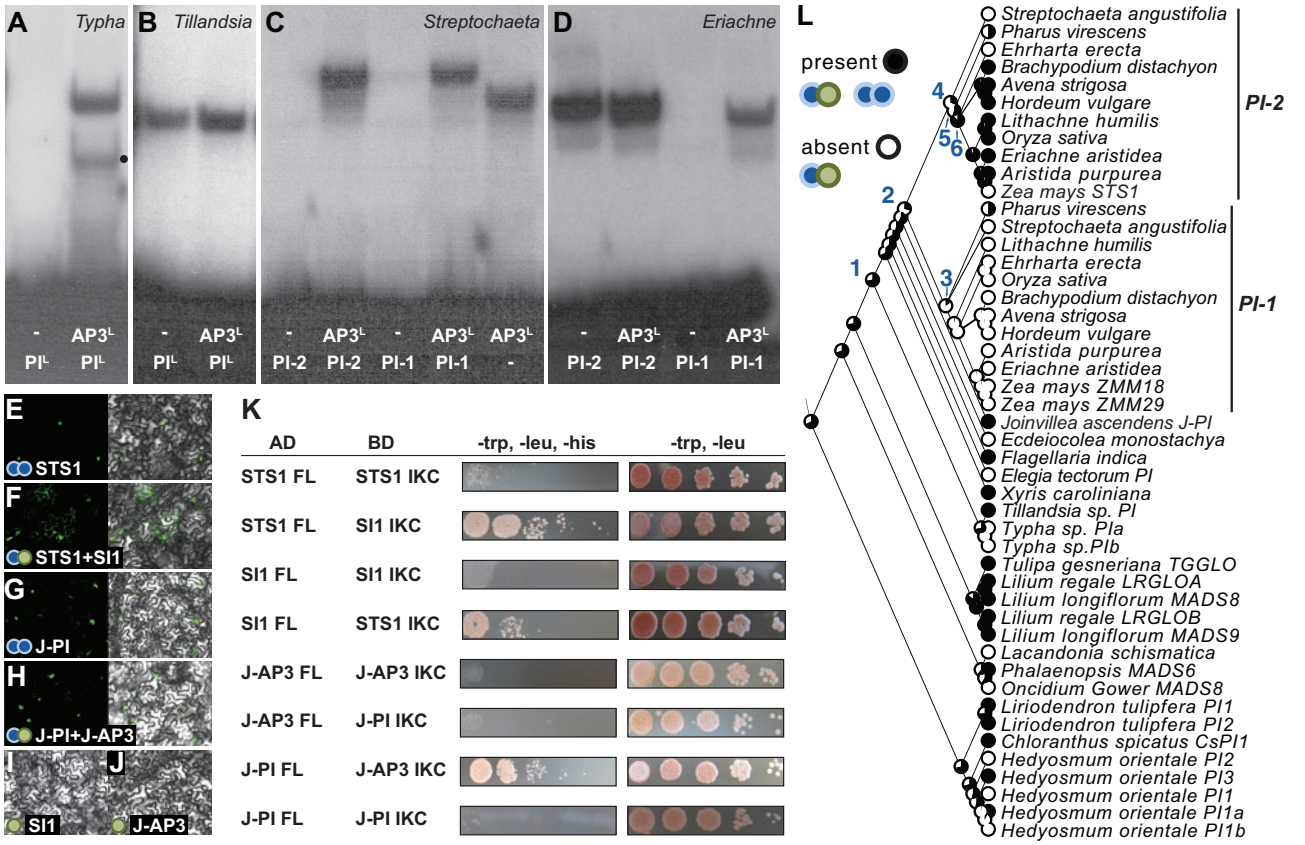

FIG. 1. PI^L dimerization patterns are evolutionarily labile in the Poales. (*A*) *Typha* PI did not homodimerize, but could form heterodimers with SI1-C. (*B*) *Tillandsia* PI can form homodimers ($AP3^L$ protein = *Ecdeiocolea* AP3). (*C*) Neither PI-1 nor PI-2 from *Streptochaeta* can form homodimers, but both can form heterodimers with *Streptochaeta* AP3. *Streptochaeta* AP3 can form DNA-binding homodimers. (*D*) PI-2 from *Eriachne* formed DNA-binding homodimers, whereas *Eriachne* PI-1 did not ($AP3^L$ protein = SI1). (*E*) BiFC assays with B-class proteins from *Joinvillea* and *Zea mays*. (*E*) STS1-YFP_N and STS1-YFP_C, (*F*) STS1-YFP_N and SI1-YFP_C, (*G*) J-PI-YFP_N and J-PI-YFP_C, (*H*) J-PI-YFP_N and J-AP3-YFP_C, (*I*) SI1–YFP_N and SI1-YFP_C (*J*) J-AP3-YFP_N and J-AP3-YFP_C, (*K*) Yeast two-hybrid assays with full-length proteins and IKC constructs. (*L*) Ancestral state reconstructions (likelihood) of dimerization states plotted onto a Bayesian phylogenetic reconstruction of PI^L genes from the Poales, as well as noneudicot taxa where PI^L dimerization has been assessed. Numbers next to the tree indicate nodes discussed in the text. •, SI1-C homodimer band.

Our gel shift assays indicated that the I-domain mediates homodimerization when swapped between J-PI and STS1, but not when swapped between BdSTS1 and STS1. A chimeric J-PI protein that contained the STS1 I-domain dimerized very weakly with J-AP3 (fig. 2B-1), but showed robust dimerization with a similar $AP3^L$ protein from *Ecdeiocolea macrostachya* (fig. 2C). In the reciprocal experiment, a chimeric STS1 protein that contained the J-PI I-domain formed homodimers (fig. 2B-2). Swapping the K-domain between J-PI and STS1 did not affect dimerization (figs. 2B-3 and *B*-4). In the BdSTS1/STS1 swaps, neither the I-swaps nor the K-swaps were sufficient to disrupt BdSTS1 homodimerization, or STS1 obligate heterodimerization (fig. 2D). These results indicate that the J-PI I-domain, but not the BdSTS1 I-domain, is sufficient to confer homodimerization on STS1. The reciprocal swaps showed that the STS1 I-domain is sufficient to abolish J-PI homodimerization, but does not affect BdSTS1 homodimerization. Thus, the molecular determinants of J-PI and BdSTS1 homodimerization are distinct, lending support to the hypothesis that PI^L homodimerization has evolved convergently in the Poales.

A Single Amino Acid Change Can Switch the Maize PI^L Protein STS1 from an Obligate Heterodimer to a Homodimer

To determine precisely which I-domain amino acid(s) mediate differential dimerization activity between STS1 and J-PI, we compared their I-domain sequences. Four amino acids differ between the STS1 and J-PI I-domains: S63T, S65P, G81D, and E82D (all residue numbers refer to STS1, STS1 residue written first). We mutated each amino acid in STS1 to the J-PI variant individually and in all possible combinations, and tested these mutagenized STS1 variants for dimerization activity (fig. 2 and supplementary table S1, Supplementary Material online). A single amino acid change, from glycine to an aspartic acid at position 81 (G81D) was sufficient to confer the ability to homodimerize on STS1 (fig. 2D-3). STS1 could be induced to bind DNA as a homodimer when G81D was changed alone, in combination with S60P and/or S63T, and when all four amino acids were changed (fig. 2E-3 and I). Furthermore, when the reciprocal change (D81G) was made to J-PI, J-PI (D81G) no longer homodimerized in gel shifts, but instead formed obligate heterodimers with J-AP3 (fig. 2F-2). Thus, a single amino acid change

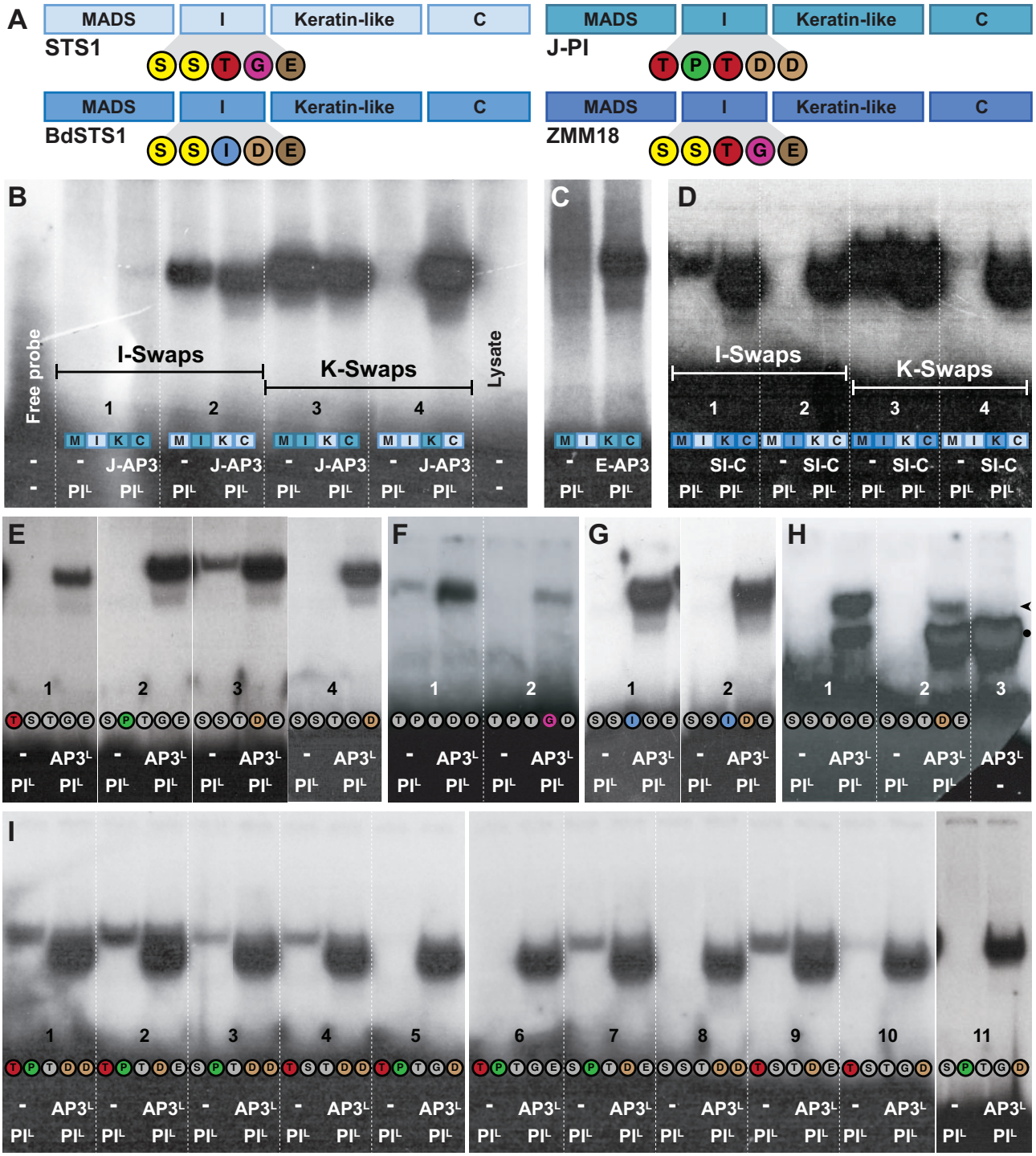

FIG. 2. A single amino acid change in the I domain is sufficient to allow STS1 homodimerization. (*A*) Domain structure of BdSTS1, J-PI, STS1, and ZMM18. The amino acids that differ between the I domains of BdSTS1, J-PI, and STS are highlighted. (*B*) J-PI and STS1 domain swaps. The $AP3^L$ protein in all lane pairs is *Joinvillea* AP3 (J-AP3). The J-PI I-domain is sufficient to confer the ability to homodimerize on STS1 (lane pair 2), and the I-domain from STS1 abolishes the ability of J-PI to homodimerize (lane pair 1). J-PI/J-AP3 heterodimerization is also negatively affected (lane pair 1). Swapping the K domains between J-PI and STS1 has no effect on dimerization capacity (lane pairs 3 & 4). (*C*) J-PI with the I domain from STS1 can interact with an $AP3^L$ protein from *Ecdeiocolea*. (*D*) BdSTS1 (*Brachypodium distachyon*) and STS1 (maize) domain swaps. Neither the I nor the K domain from STS1 is sufficient to disrupt BdSTS1 homodimerization. The $AP3^L$ protein in all lanes is SI1-C. (*E*) STS1 mutagenesis at single sites. G81D (lane pair 3) is sufficient to allow STS1 homodimerization. $AP3^L$ in lane pair 1 is SI1-C. The $AP3^L$ protein in lanes pairs 2-4 is J-AP3. (*F*) The reciprocal change on J-PI (D81G) is sufficient to disrupt J-PI homodimerization in favor of obligate J-PI/J-AP3 heterodimerization. (*G*) T73I disrupts the ability of STS1(G81D) to form homodimers. The PI^L protein in lane pair 1 is STS1(T73I), in lane pair 2 it is STS1(T73I + G81D). The $AP3^L$ protein in both lane pairs is SI1-C. (*H*) The G81D mutation does not promote ZMM18 (G81D) homodimerization. SI-C forms homodimers in gel shifts (lower band), but migrates faster than ZMM18/SI-C heterodimer (at arrowhead, top band in lane pairs 1 & 2). (*I*) STS1 mutagenesis in all possible combinations. $AP3^L$ construct in (*F*), and (*G*) is SI1-C. •, SI1-C homodimer band.

(G81D) in the I-domain is sufficient to confer the ability to homodimerize on STS1.

Curiously, the BdSTS1 I-domain contains an aspartic acid at position 81, but the BdSTS1 I-domain was not sufficient to confer the ability to homodimerize on STS1 (fig. 2D). This led us to hypothesize that other residues in the BdSTS1 I-domain, in addition to residue 81, influence B-class dimerization patterns. BdSTS1, J-PI, and STS1 differ in that BdSTS1 contains an isoleucine at position 73 (threonine in J-PI and STS1), unique among grass PI^L proteins. In order to determine whether the identity of the residue at position 73 had an effect on dimerization, we mutated it in STS1, and in STS1(G81D). STS1(T73I) and STS1(T73I + G81D) both formed obligate heterodimers with $AP3^L$ proteins (fig. 2G). Thus, it is only in combination with the precise background protein sequence of STS1 that G81D is sufficient to confer the ability to homodimerize on STS1.

Similarly, the ability of G81D alone to influence dimerization is specific to STS1, and does not extend to the maize PI-1 protein ZMM18. All maize PI^L proteins contain a glycine at position 81, however ZMM18 (G81D) still bound DNA as an obligate heterodimer with SI1 in gel shifts, albeit somewhat weaker than with the unmutagenized proteins (compare top band in fig. 2H-1 and *H*-2). Taken together with our domain swap experiments, this demonstrates that the affect of G81D on B-class protein dimerization is context-dependent. In addition, these results show that the molecular determinants of homodimerization versus obligate heterodimerization in STS1 and ZMM18 are distinct. Along with our ancestral state reconstructions, this indicates that STS1 obligate heterodimerization evolved independently from the obligate heterodimerization characteristic of the maize PI-1 proteins.

Obligate Heterodimerization of STS1 with SILKY1 Evolved Very Recently

The question remained whether obligate heterodimerization evolved along the branch leading to STS1 (maize), or whether obligate $PI^L/AP3^L$ heterodimerization was characteristic of B-class proteins from a number of taxa, more closely related to maize than what we included in our assays. The glycine at position 81 that mediates STS1 hetero- versus homodimerization is present in all maize PI^L proteins, but not in any other PI^L proteins in our data sets (supplementary figs. S3 and S5, Supplementary Material online). Although this result suggested that obligate heterodimerization evolved recently, our sampling did not allow us to assess exactly when obligate heterodimerization arose in the PI-2 clade. To address this question, we took advantage of the extensive genetic and genomic resources in maize. The maize HapMap2 project characterized genetic variation across 60 improved maize lines, 23 maize landraces, 19 wild relatives (teosintes), and 1 representative of the sister genus, *Tripsacum dactyloides* (Chia et al. 2012). The nucleotide change that ultimately results in a transition from D (Asp) to G (Gly) at position 81 in STS1 was characterized by the HapMap2 project (G/A, Chr3, position 171,472,161, AGPv3). This causative single nucleotide polymorphism (SNP) is one of four *STS1* missense polymorphisms in the HapMap2 data set, but the other three are all toward the C-terminus of the K domain, and not likely contributors to hetero- versus homodimerization. The G81 allele (G at nucleotide position 241) was fixed in 78/78 maize lines genotyped at this position. In teosinte the D81 allele (A at nucleotide position 241) was found in the heterozygous condition in one line, whereas the remaining 16 of 17 teosinte lines genotyped at this position had the G81 allele (G). The tested accession of *T. dactyloides* was homozygous for the D81 allele (A). These results indicate that the D81G change that contributed to the evolution of obligate heterodimerization of STS1 occurred along the branch leading to maize and teosinte, and became fixed in maize, possibly during the bottleneck of domestication. Thus, phylogenetic, biochemical, and population genetic data combined all indicate that obligate heterodimerization of STS1 evolved very recently, in large part because of a shift from aspartic acid to glycine at residue 81.

Positive Selection Acting on PI-2 Residues Predicted to Be Involved in PPIs

Gene duplications, such as the duplication that led to the *PI-1* and *PI-2* gene clades, are hypothesized to precede gene neo- or subfunctionalization in some cases (Lynch et al. 2001). Neo- or subfunctionalization may leave a signature of codon diversification or directional evolution that can be detected using computational tests (Yang and Bielawski 2000; Kosakovsky Pond and Frost 2005b). In the case of the evolution of PI^L dimerization, we expected short bursts of diversifying or directional selection acting on individual branches and sites, rather than persistent, diversifying selection (e.g., Hughes and Nei 1988; Renner and Specht 2012). In particular, we hypothesized that positive selection might have acted along the branch leading to the PI-2 clade of genes in the grasses, or along the branch leading to node 6 (fig. 1L). We employed multiple tests to detect either periodic diversifying (branch-sites random effects likelihood [REL], branch-sites Bayes Empirical Bayes [BEB] tests) or directional selection acting on specific branches and sites (model of episodic directional selection [MEDS]), or directional selection acting on sites in a phylogeny (directional evolution of protein sequence [DEPS] and FUBAR approach to directional evolution [FADE]) (Pond et al. 2005; Kosakovsky Pond and Frost 2005a; Yang 2007; Kosakovsky Pond et al. 2008, 2011; Murrell et al. 2012).

We identified residues under either directional or diversifying selection acting on the branch leading to the PI-2 clade, or within the PI-2 clade, in all but one test (branch-sites REL) (fig. 2M and supplementary fig. S5 and table S2, Supplementary Material online). Our results were robust to differing sampling and multiple runs. Our selection test results likely differ from previous reports (Mondragon-Palomino et al. 2009; Wei and Ge 2011) because of different sampling, different tests employed, and differing model choices (Zhang et al. 2005). We focused on six sites identified as experiencing positive selection, particularly directional selection, by at least two tests (table 1). Five of these six sites occur in interaction motifs (fig. 3A), previously identified as key mediators of Arabidopsis MADS-box PPIs (van Dijk et al. 2010). Thus, we detected a signal of positive selection acting on amino acid residues in PI^L proteins, preferentially located

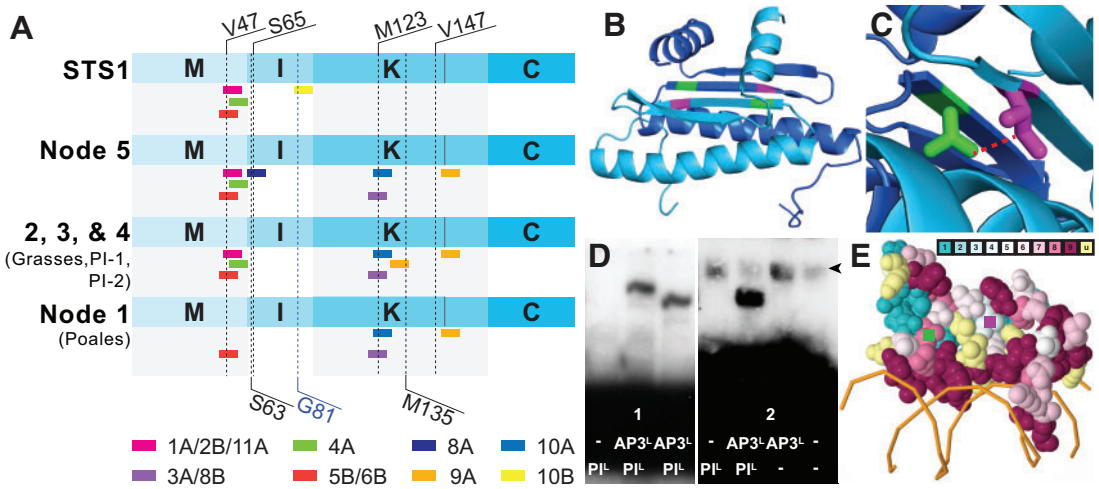

Fig. 3. Positively selected residues are preferentially clustered in interaction specificity motifs, and the identity of residue 47 can affect PI^L dimerization. (*A*) Residues predicted to be under positive selection are preferentially clustered in interaction motifs (Van Dijk et al, 2010), indicated by black dotted lines. The position of G81, key in mediating STS1 dimerization, is shown in blue. (*B*) Homology model of a dimer of proteins from node 5. The highly conserved valine at position 43 is shown in green, the more variable residue at position 47 (valine or isoleucine) is pink. (*C*) The isoleucine at position 47 in the node 5 ancestral protein is close enough to interact with val43 in B-class dimerization. (*D*) The identity of residue 47 can effect PI^L dimerization. When the STS1 I-domain is combined with I47V mutagenesis, BdSTS1 homodimerization is disrupted (lane 1-1). The chimeric protein can still form heterodimers with *Brachypodium* AP3 (lane 1-2) and SI1-C (lane 1-3). BdSTS1 homodimerization is also disrupted if only the I47V and D81G changes are made (lane 2-1). BdSTS1(I47V + D81G) forms obligate heterodimers with SI1-C. Arrowhead points to artIfact band in the lysate control. (*E*) Conservation (ConSurf) scores of PI^L proteins from the Poales, shown on a model of MEF2. Scores range from 0 to 9. u, undefined. Green square = conserved residue 43, Pink square = variable residue 47.

Table 1. Amino Acid Residues under Selection, as Detected Using Multiple Methods.

Residue (STS1)[a]	BEB[b]	MEDS[b] (aa)	DEPS[b] (aa)	FADE[b] (aa)	Domain	PPI[c]	Motif
47(V)		0.00089 (V)	489 (V)	1 (V)	M	Dimerization	11A, 1A, 2B
63 (S)			1792.2 (S)	1 (S)	I	N/A	8A
65(S)		0.00167 (S)	102.6 (S)	0.99 (S)	I	N/A	8A
123(M)	0.89–0.99	0.00871 (M)			K	None predicted	10A, 8B, 3A
135(L)		0.00087 (V)	192.2 (V)		K	Dimerization	9A
147(V)	0.94–0.99		172.2 (V)	0.99 (V)	K	Tetramerization	None

[a]Position and amino acid identity are in parentheses all for STS1.
[b]MEDS analysis, *P* values are shown. DEPS analysis, Bayes Factors are shown. Bayes Empirical Bayes and FADE analyses, posterior probabilities are shown. Target amino acids in tests for directional selection are shown in parentheses.
[c]Predicted to contact another chain in a PPI in homology models. Residues 63 and 65 are outside of regions that can be reliably modeled.

in motifs known to influence MADS-box PPI specificity, associated with the gene duplication event that led to the *PI-1* and *PI-2* gene clades.

To address whether any residues under positive selection were likely involved in PPIs, we used homology modeling. No crystal structures of full-length MIKC MADS-box protein have been reported; however, crystal structures of (nonplant) MADS-domain dimers and K-domain tetramers from SEP3 have been determined (Pellegrini et al. 1995; Tan and Richmond 1998; Santelli and Richmond 2000; Puranik et al. 2014). We used the SWISS-MODEL server to identify the best templates for modeling, and built MADS-domain and K-domain homology models for STS1 and the predicted ancestral sequences at nodes 2, 4, and 6 (Arnold et al. 2006; Biasini et al. 2014).

Four of the six positively selected residues identified by more than one test were in protein regions that could be modeled with high confidence, and three of those four were predicted to be involved in PPIs (table 1). The closest homolog with resolved MADS domain dimer crystal structures is mammalian MEF2 (55.88% homology). We used two independent MEF2 crystal structures in our homology modeling experiments (Santelli and Richmond 2000; Jayathilaka et al. 2012;). Our MADS-domain homology models predict that residue 47 is one site of interchain interaction in PI-2 MADS dimer formation. The amino acid at position 47 is consistently involved in a hydrophobic interaction with a highly conserved valine at position 43 of the other monomer (fig. 3B and *C*). Thus, the identity of the residue under selection at position 47 might affect B-class PPIs. Similarly, when we used a recent SEP3 crystal structure (28–35% homology) (Puranik et al. 2014) to model the K-domains of both extant and reconstructed ancestral proteins from the grasses, residue 135 was consistently involved in dimerization. In addition, residue 147 was predicted to be involved in tetramerization of the ancestral protein reconstructed at node 4, and of STS1.

Thus, three of four positively selected amino acids that could be reliably placed in a structural homology model are likely directly involved in interactions between MADS monomers and dimers. These data, taken together, indicate that the signal of positive selection we detected acting on PI^{L} proteins in the grasses may indeed be associated with the evolution of PPIs.

Altering a Positively Selected MADS-Domain Amino Acid Residue Can Change B-Class Dimerization

To test whether the identity of positively selected residues could affect dimerization in vitro, we performed further site-directed mutagenesis experiments with PI-2 proteins. We chose to investigate residue 47 because it was predicted to be under directional selection, could be modeled reliably, and changed within the PI-2 clade. STS1 has a valine at residue 47 in all genotyped maize and teosinte accessions, and in *T. dactyloides* (Chia et al. 2012). In contrast, the *B. distachyon* STS1 ortholog (BdSTS1), and the predicted ancestral sequences at nodes 2, 3, 4, 5, and 6 all have an isoleucine at position 47. The STS1 I-domain was not sufficient to disrupt BdSTS1 homodimerization (fig. 1D-1). However, when we changed I47 to valine in addition to the I-domain, this chimeric protein no longer formed homodimers (fig. 3D-1). Similarly, when BdSTS1 residues 47 and 81 were changed to the maize variants (BdSTS1 [I47V + D81G]), the mutagenized protein could no longer form homodimers (fig. 3D-2). Both mutagenized proteins still formed heterodimers with AP3^{L} proteins. Similar to G81D, although the identity of residue 47 was critical in determining homodimerization potential in the context of BdSTS1, a valine at position 47 is not completely linked to obligate heterodimerization. Val47 is found in a number of PI^{L} proteins that form homodimers (e.g., *Avena sativa* PI-2; supplementary fig. S5, Supplementary Material online). However, our results show that the identity of the positively selected residue at position 47 contributes to the dimerization landscape of grass PI^{L} proteins.

Patterns of Sequence Conservation Differentiate Modules within PI^{L} Proteins

Changes to protein-coding regions are thought to have a higher potential for negative pleiotropic effects than changes to noncoding regions (Carroll 2000; Stern 2000). Nonetheless, we found evidence for coding evolution in the Poales, under positive selection, and with demonstrated consequences to PPIs (fig. 3). We hypothesized that substitutions affecting core protein function (i.e., DNA binding) have the potential to severely impact protein function, and therefore may have experienced different selective pressures than substitutions affecting PPIs. To explore variable signatures of selection acting on PI^{L} proteins in the context of protein structure, we used the ConSurf webserver. ConSurf can be used to assess patterns of sequence conservation within an alignment, and transfer that information to a homology model (Landau et al. 2005). ConSurf sequence conservation scores for each position in an alignment range from 1 (extremely variable) to 9 (highly conserved). We found that amino acids potentially important for B-class dimerization specificity and/or under positive selection occurred in weakly to moderately conserved regions of PI^{L} proteins. For example, residue 47, which is under positive selection and involved in variable dimerization, had a relatively low ConSurf score of 4. Furthermore, most amino acids predicted to be critical for DNA binding are deeply conserved in PI^{L} proteins with high Consurf scores between 7 and 9 (fig. 3E). This result underscores the modular architecture characteristic of the MIKC MADS-box transcription factors, and indeed of many proteins (Kaufmann et al. 2005; Hoekstra and Coyne 2007; Bartlett and Whipple 2013). Changes to the DNA-contacting amino acid residues that would presumably be detrimental to core protein function are selected against. Consequently, these residues are more likely to remain invariant over evolutionary time and have high conservation scores. In contrast, the regions of PI^{L} proteins that modify PPIs are under less stringent selection, possibly allowing for shifting interactions over evolutionary time. This modularity and variability in selective pressure means that some classes of structural change have less capacity for negative pleiotropy than others (Lynch and Wagner 2008; Bartlett and Whipple 2013).

J-PI and STS1 Show Similar Rescue of B-Class Mutants

The question remained as to what function, if any, PI^{L} homodimers from the Poales have *in planta*. We turned to a rapid, heterologous transformation system to assess the function of a PI^{L} homodimer *in planta*. Specifically, we expressed J-PI under the control of the *AP3* promoter in Arabidopsis using the pOp/LhG4 transactivation system (Baroux et al. 2005), and assayed the ability of J-PI to rescue putative null alleles of *AP3* and *PI*. Arabidopsis *AP3* expression is confined to whorls 2 and 3 early in development, and is expressed at low levels in adult sepals. Arabidopsis *PI* expression is similar, except that it is also expressed in whorl 4 early on in floral development (Goto and Meyerowitz 1994; Schmid et al. 2005). When J-PI was expressed in *pi-1* mutants, (*pi-1; pAP3::Lhg4* ≫ *10-Op::J-PI*), first whorl sepals were petaloid (fig. 4C), and second whorl petals appeared normal. Third and fourth whorl organ rescue was more variable. The *J-PI* rescue lines had a mix of hybrid stamenoid–carpeloid organs, bare filaments, carpels, small abortive stamens, and almost completely normal stamens in the third whorl. The increase in total organ number in *J-PI* rescue lines was statistically significant (*t*-test, $P < 0.05$). *J-PI* also rescued other *pi-1* phenotypes including gynoecium defects and third and fourth whorl fusion defects (fig. 4I and *J*). *J-PI*, expressed under the *pAP3* promoter, did not rescue *ap3-4* mutants (seven independent transgenic lines).

We attained very similar results in a *pi-1* and *ap3-4* mutant lines expressing *STS1* under the *AP3* promoter (supplementary fig. S6, Supplementary Material online). Our *STS1 pi-1* rescue results recapitulated those of Whipple et al. (2004), where *STS1* was also expressed under the Arabidopsis *AP3* promoter, and caused petaloid sepal margins. Both the *J-PI* and the *STS1 pi-1* rescue lines strongly resembled those where Arabidopsis *AP3* or *PI* was ectopically expressed in flowers, under the 35S promoter (Krizek and Meyerowitz 1996a; Yang, Xiang, et al. 2003). *STS1*, expressed under the *pAP3* promoter, did not rescue *ap3-4* mutants (two independent lines). In summary, both J-PI and STS1 showed similar rescue of the

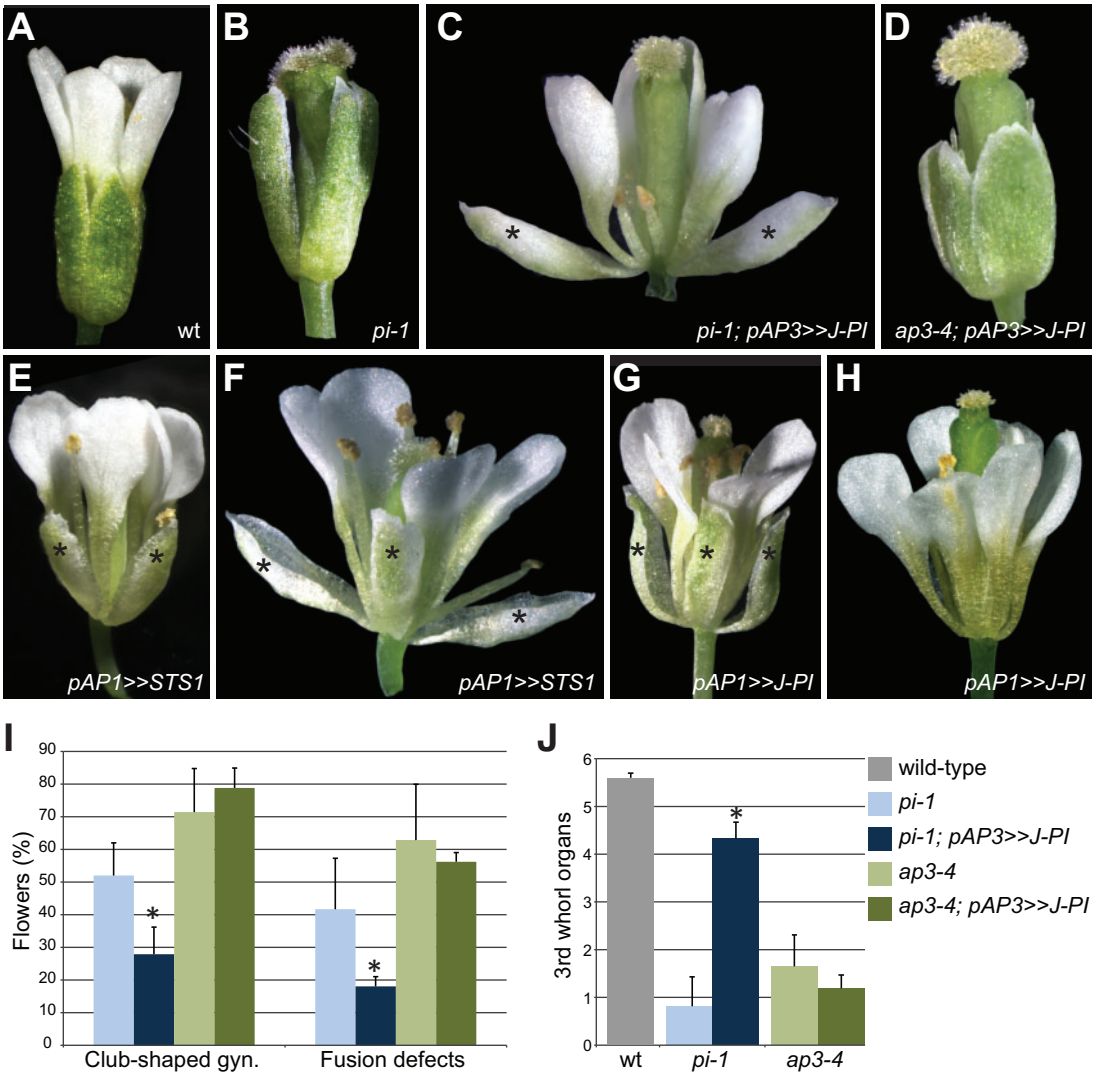

Fig. 4. Heterologous expression of J-PI homodimers and obligate STS1 heterodimers in *Arabidopsis thaliana*: (*A*) Wildtype Arabidopsis flower, (*B*) *pi-1* mutant, (*C*) *J-PI* under the *AP3* promoter (*pAP3::LhG4 ≫ 10-Op::J-PI*) showing partial rescue of the *pi-1* mutant phenotype. Sepals (marked with *) are petaloid (closest sepal removed). (*D*) The same *J-PI* construct under the *AP3* promoter (*pAP3::LhG4 ≫ 10-Op::J-PI*) does not rescue the *ap3-4* mutant phenotype. (*E*, *F*) Transformants expressing *STS1* under the *AP1* promoter (*pAP1::LhG4 ≫ 10-Op::STS1*) exhibit petaloid sepals. Transformants expressing *J-PI* under the *AP1* promoter (*pAP1::LhG4 ≫ 10-Op::J-PI*) either show petaloid sepals (*G*), or the complete homeotic transformation of sepals into petals (*H*). (*I*, *J*) Quantification of *J-PI* rescue of *ap3-4* and *pi-1* mutants. *J-PI*, under the *AP3* promoter, partially rescued the club-shaped gynoecium phenotype, as well as the fusion and organ number defects typical of the *pi-1* mutant. Neither club-shaped gynoecia nor fusion defects were observed in wildtype flowers.

pi-1 mutant phenotype, where they were presumably acting as part of complexes with AP3 (Whipple et al. 2004; Whipple and Schmidt 2006). In addition, neither J-PI nor STS1 conferred B-class function without an AP3 partner as neither J-PI nor STS1 could rescue *ap3-4* mutants.

The J-PI Homodimer Can Transform Arabidopsis Sepals into Petals

Altered interactions between MADS-box proteins from snapdragon, in conjunction with variable expression patterns, have the capacity to effect phenotypic change in Arabidopsis (Airoldi et al. 2010). This led us to ask whether the J-PI homodimer, when expressed at high levels in a new domain, could induce novel phenotypes in Arabidopsis, distinct from those induced by STS1. To this end, we again used the pOp/LhG4 transactivation system (Baroux et al. 2005), this time to drive high expression of *J-PI* and *STS1* in developing sepals, using the Arabidopsis *AP1* promoter. *AP1* is initially expressed throughout the floral meristem, but is only detected (using in situ hybridization) in the first (sepal) and second (petal) whorls by the time sepal primordia become evident (Mandel et al. 1992).

Ectopic expression of *STS1* in developing sepals (4/4 lines) resulted in first whorl sepal margins that became slightly petaloid, similar to what was observed under the *AP3* promoter (fig. 4E and *F*). In contrast, ectopic expression of *J-PI* in Arabidopsis sepals resulted in the complete transformation of the first whorl organs into petals indistinguishable from second whorl petals (6/11 independent transformation lines) (fig. 4H). These homeotically transformed organs resembled

sepals ectopically expressing both AP3 and PI (Krizek and Meyerowitz 1996a). Similarly, when a version of AP1 that has strong transactivation potential is ectopically expressed in Arabidopsis sepals, they are also transformed into petals, probably because of the ectopic upregulation of both *AP3* and *PI* (Ng and Yanofsky 2001; Lamb et al. 2002). In 5 of the 11 *J-PI* lines, sepals resembled those of *pAP1* ≫ *STS1* transformants with stronger phenotypes. In strong *pAP1* ≫ *STS1* lines (2/4 independent lines), sepals had petaloid margins but were not completely transformed (fig. 4G). Our results with STS1 were similar to those seen with ectopic expression of Arabidopsis *PI*, or the *Petunia hybrida* $AP3^L$ gene *green petals* in all four whorls of the Arabidopsis flower (under 35S, both obligate heterodimers; Halfter et al. 1994; Krizek and Meyerowitz 1996a; Yang, Xiang, et al. 2003). These results show that J-PI, when expressed at a high level in a novel domain, differs from STS1 in its effects on floral development.

Discussion

The PPI landscape of any gene product is a critical component of function. In plant development, there are myriad examples of regulatory PPIs central to the development of individual traits and organs (e.g., Sabatini et al. 2003; Cui et al. 2007; Kanaoka et al. 2008; Lau et al. 2014). Changing these interactions over evolutionary time is one hypothesized way to achieve regulatory diversity, without negatively affecting core protein function (Lynch and Wagner 2008; Tuch et al. 2008). We identified a pattern of unexpected evolutionary lability in B-class MADS-box PPIs in the Poales. Within the grasses, obligate $AP3^L$/PI^L heterodimerization has evolved from PI^L homodimerization at least twice. The evolution of obligate heterodimerization of the maize protein STS1 appears to have occurred very recently: The causative SNP was fixed during domestication. We detected a signal of positive selection acting on residues predicted to be involved in PPIs, one of which has an effect on PI^L protein dimerization. We also showed that heterologous expression of Poalean MADS-box proteins, which differ in their PPI spectra, can affect floral form in Arabidopsis.

Shifting B-Class PPIs and Evolutionary Change in the Poales

Given our sampling in an extremely speciose family and order, the examples of shifts described here are almost certainly an underestimate. This is in stark contrast to what has been reported in the core eudicots, where B-class homodimers are rare (summarized in Melzer et al. 2014). In the monocots outside of the Poales, in the early-diverging angiosperms, and in the noncore eudicots there appears to be more lability and more frequent B-class homodimerization (summarized in Melzer et al. 2014), but it is hard to assess the degree of change without more fine-grained sampling. Obligate B-class heterodimerization has been connected to the evolution of the highly canalized flowers typical of the core eudicots, where there is almost no intergradation between floral organs of different types (Winter et al. 2002; Lenser et al. 2009; Specht and Bartlett 2009; Melzer et al. 2014). The evolutionary lability we have found in the Poales, as well as the presence and maintenance of PI^L homodimerization in lineages like the grasses, which on the whole possess highly canalized flowers (Kellogg 2015), argues against this idea. Instead, our results suggest that obligate B-class heterodimerization in particular is not necessary for the tight maintenance of separate floral whorls, and may serve another function, or indeed no function at all, particularly in the Poales.

Within the Poales, there are suggestive associations between dimerization state and floral and inflorescence morphology. In nongrass Poaleans, we observed obligate heterodimerization more often in taxa that are wind pollinated. *Ecdeiocolea*, *Elegia*, and *Typha* are all wind pollinated, and all show obligate B-class heterodimerization. In contrast, *Flagellaria*, *Joinvillea*, *Tillandsia*, and *Xyris* are all probably animal pollinated, and all of their PI^L proteins can form homodimers (pollination states summarized in Givnish et al. 2010). The morphological wind pollination "syndrome" often includes a reduced perianth, anthers on long flexuose filaments, and/or unisexual flowers (Linder 1998; Culley et al. 2002). In addition, wind pollination evolves in a correlated way with traits that could be linked to B-function, including floral showiness (often associated with perianth characteristics) and floral sexuality (Friedman and Barrett 2008). Thus, some of the morphological traits thought to favor wind pollination include modifications to second and third whorl organs, which are often specified by B-class gene function. Within the grasses, PI^L homodimerization may have emerged coincident with the origin of lodicules and the specialized grass spikelet (node 4), or coincident with a major diversification event that led to the hyperdiverse BEP and PACMAD grass clades (node 6). Although our sampling is far from complete, and it is unwarranted to connect cause and effect, these patterns are intriguing and may be indicative of a connection between morphology and B-class dimerization in the Poales.

Just as the shifting PPIs we have uncovered may be connected with morphological evolution in the Poales, they may also underlie phenotypic conservation. For example, in "developmental systems drift," the regulatory architecture underlying a particular phenotype may change considerably, but the phenotype itself may remain stable (True and Haag 2001). An excellent example of this phenomenon is the nematode vulva. Although formed from the same three cells in both *Caenorhabditis elegans* and *Pristionchus pacificus*, vulva development is controlled by divergent genetic pathways in the two species (Sommer 2012). In the Poales, the regulatory architecture of floral development may differ drastically between species, but floral development may ultimately proceed along similar lines across the order. In an allied concept, floral development in the Poales may be robust to underlying genotypic change, and shifting B-class PPIs. Robustness allows for the accumulation of cryptic genetic variation, which in some cases can serve as raw material for natural selection, resulting ultimately in rapid phenotypic change (Wagner 2011, 2005; Paaby and Rockman 2014). For the B-class genes in particular, robustness has been suggested to be derived from partial to complete redundancy between duplicates in a genome, particular PPIs, and regulatory relationships

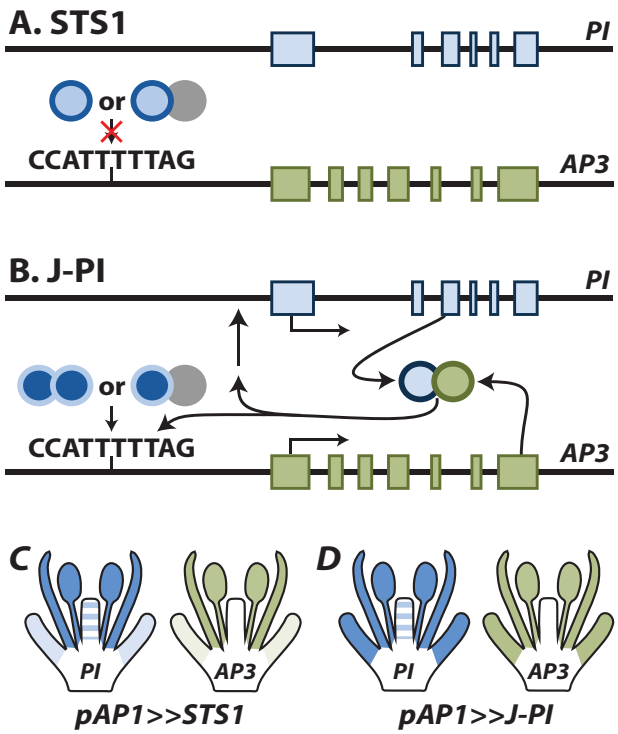

FIG. 5. A model of STS1 and J-PI action in Arabidopsis flowers expressing either *STS1* or *J-PI* under the *AP1* promoter. (*A*, *C*) STS1, either alone or in complex with other Arabidopsis proteins, does not bind the *AP3* promoter or activate high levels of *AP3* or *PI* expression in sepals. (*B*, *D*) J-PI, as a homodimer and/or in complex with other Arabidopsis proteins, can bind the *AP3* promoter and, in turn, activate high expression of both *AP3* and *PI*. This ectopic B-class expression triggers the homeotic transformation of the sepals into petals in *J-PI* expression lines, but not *STS1* expression lines.

between B-class genes (Lenser et al. 2009; Geuten et al. 2011). In the Poales, the lability we have uncovered may represent a small fraction of the molecular divergence underlying robust floral developmental pathways.

PI^L Gene Function Has Changed in the Grasses, Concomitant with Shifting PPIs

The signature of positive selection we detected acting on residues that mediate PPIs of one PI^L paralog in the grasses may indicate sub- or neofunctionalization of the two grass PI^L genes. There is evidence for functional differentiation of the two PI homologs in rice (Kang et al. 1998; Kyozuka et al. 2000; Yadav et al. 2007), which differ in their ability to homodimerize (fig. 2L and supplementary fig. S1, Supplementary Material online). The two rice PI^L homologs, OsMADS2 and OsMADS4 are expressed in essentially the same domains, but OsMADS2 (or the OsMADS2/SPW1 heterodimer) has a particular role in second whorl organ (lodicule) development (Kang et al. 1998; Nagasawa et al. 2003; Prasad and Vijayraghavan 2003; Yao et al. 2008). Gene function has also diverged within the *PI-2* clade, again associated with changing PPIs. In contrast to rice *OsMADS2*, *STS1* function is not limited to lodicule identity (Bartlett et al. 2015). *OsMADS4* and *STS1* have very similar expression patterns (Kyozuka et al. 2000; Munster et al. 2001; Whipple et al. 2004, 2007). Thus, the functional differences between *OsMADS4* and *STS1* may be due to altered PPIs. In addition, the regulatory relationships between rice B-class genes are distinct from those seen between the B-class genes of maize. In maize, *STS1* shows no redundancy with *ZMM18* or its close paralog, *ZMM29*, likely because *ZMM18* and *ZMM29* require the STS1/SI1 heterodimer to initiate their expression (Bartlett et al. 2015). In contrast, knockdowns of rice *OsMADS2* and *OsMADS4* do not affect expression of other B-class genes (Prasad and Vijayraghavan 2003; Yao et al. 2008). This suggests that STS1 and OsMADS2 have diverged not only in dimerization potential and homeotic function but also in their roles within the floral development gene regulatory landscape. Functional differentiation of B-class proteins is associated with altered PPIs in a number of lineages (Kang et al. 1998; Prasad and Vijayraghavan 2003; Vandenbussche et al. 2004; de Martino et al. 2006; Geuten and Irish 2010). In the grasses, we have found a similar relationship between altered B-class PPIs, and changing gene function.

Changing PPIs and Functional Change

Evolutionary changes to core protein function, like altered DNA-contacting or active-site residues, have the potential to eliminate protein function. Regulatory proteins often have multiple roles in different developmental contexts, and altering DNA-binding has the potential to change all of these roles (negative pleiotropy). Thus, coding changes to DNA-binding domains are thought to be, and are in our analyses, under strong negative selection (Stern and Orgogozo 2008). In contrast, evolutionary changes in residues affecting PPIs may be under less stringent selection and allow for the evolution of new protein function (Lynch et al. 2008; Tuch et al. 2008). Consistent with this hypothesis, we found evolutionary change in B-class dimerization across the Poalean phylogeny (fig. 2L). Residues in Poalean PI^L proteins likely directly contacting DNA are deeply conserved, whereas residues involved in dimerization show more evolutionary variability (fig. 3E). Not all coding changes have the same potential for negative pleiotropy or for affecting functional divergence. Changing PPIs, in particular, may be one class of structural change that allows for novel protein function, while avoiding some of the pitfalls inherent to changing deeply conserved protein function, like DNA-binding specificity.

The J-PI Homodimer Differs from STS1 in Its Effects on Floral Development in Arabidopsis

Although the J-PI homodimer could not rescue the *ap3-4* mutant, ectopic expression of J-PI in sepals (using the *AP1* promoter) was sufficient to promote the homeotic transformation of sepals to petals. In contrast, we never observed this complete transformation with STS1, which forms obligate heterodimers with $AP3^L$ proteins. Instead, ectopic *STS1* expression resulted in slight petaloidy of the sepals, similar to that observed when *PI* is ectopically expressed in *Arabidopsis thaliana* sepals (fig. 5; Krizek and Meyerowitz 1996a; Yang,

Xiang, et al. 2003). In contrast to our results, the ectopic expression of a homodimerizing PI^L protein from *Lilium longiflorum* resulted in slight petaloidy at sepal margins, rather than complete transformation of sepals into petals (Chen et al. 2011). These differing results may be due to different promoters used (*pAP1* vs. 35S), or the homeotic transformation we observed may not be the direct result of hetero-versus homodimerization. In addition to differential dimerization patterns, J-PI and STS1 may bind different DNA sequences, and/or J-PI and STS1 may differ in their ability to interact with other Arabidopsis MADS-box proteins, including AP3. As our homology models suggest that the J-PI and STS1 residues most likely to contact the DNA are identical, we favor the hypothesis that any potential differences in DNA-binding activity between J-PI and STS1 are because of divergent PPIs or protein–cofactor interactions. These results support our overall hypothesis that differing PPIs, in conjunction with a novel expression domain, can alter protein function and organismal phenotype (fig. 4).

We integrated our results into a model to explain J-PI's function in Arabidopsis (fig. 5). The J-PI homodimer does not have the capacity for full homeotic function and cannot rescue the *ap3* mutant (fig. 4D). Although STS1 cannot bind the *AP3* promoter without an AP3 partner, the J-PI homodimer can bind the *AP3* promoter in vitro (the probe used in our EMSAs is derived from *pAP3*). This J-PI binding may upregulate *AP3* expression in the sepals of the *pAP1≫J-PI* lines. This ectopic AP3 can form heterodimers with J-PI (Whipple and Schmidt 2006), or PI itself, which is weakly expressed in older sepals (Schmid et al. 2005), and go on to homeotically transform the sepals into petals. Thus, a novel protein complex that includes the J-PI homodimer, expressed in a new domain, could have the capacity to affect floral morphology in significant ways.

Coding and Noncoding Changes Both Impact the Evolution of Gene Function

It was only in the context of high expression in Arabidopsis sepals that we saw a difference between heterologous expression of *J-PI* and *STS1* (under the *AP1* promoter). This interplay between PPIs and gene expression patterns has been demonstrated in studies of both evolutionary and developmental biology (Melzer and Theißen 2009; Smaczniak, Immink, Muino, et al. 2012; Davies and Bergmann 2014; Jetha et al. 2014; Furumizu et al. 2015). For example, altered PPIs overlaid on existing interactor expression domains contribute to the functional divergence of snapdragon C-class function (Airoldi et al. 2010). A changing PPI does not occur in isolation. Changes to PPIs are always overlaid on the expression pattern of the protein in question, and the expression patterns of all of its interactors. Although this layering of complexity can make dissecting the functional effects of evolutionary change challenging, it also provides a mechanism for amplifying small changes that might otherwise be neutral. The J-PI homodimer on its own is not sufficient to confer homeotic B-class function in Arabidopsis, but a novel protein complex in a novel domain can effect phenotypic change.

Conclusion

We have shown evolutionary lability in PI^L dimerization in the Poales, associated with functional differentiation and positive selection. We identified individual amino acids that change across the tree and mediate PI^L dimerization, and we have shown that altered PPIs have the potential to effect phenotypic change under certain circumstances. The precise role of changing B-class PPIs in the regulation of floral development and the evolution of morphological diversity in the Poales remains an open question. Our results highlight the need for functional characterization of B-class hetero- versus homodimers in the organisms in which they occur.

Materials and Methods

Assessment of PPIs

Full-length PI^L genes were amplified from taxa spanning the Poales using a combination of primers in conserved gene regions, primers in conserved upstream noncoding sequences, and 3′-RACE (Rapid Amplification of cDNA Ends) (supplementary table S3, Supplementary Material online). The full-length cDNAs were subcloned into the expression vector pSPUTK for use in EMSAs. EMSAs were performed as previously described (Whipple et al. 2007). Clones for Y2H assays were generated by amplifying full length or truncated cDNAs and inserting into the pENTR d-TOPO entry vector (Life Technologies), followed by recombination into GAL4 DNA binding domain (pGBKT7) or activation domain (pGADT7) converted to Gateway destination vectors. Correct clones were transformed into the PJ69-4a (pGBKT7) and pJ69-4α (pGADT7) yeast strains, and mated to generate diploid yeast. For BiFC assays, full-length cDNAs lacking a stop codon were cloned into a pBJ36 derivative containing either the N- or the C-terminal of YFP, then subcloned into the Not1 site of the pMLBART27 binary vector. BiFC experiments were performed as described in Gallavotti et al. (2011), and imaged 60 h after initial infection using a Olympus FluoView FV1000 confocal laser scanning microscope. Constructs with only the N- or the C-terminal of YFP were coinfected as negative controls.

Phylogenetic Analysis, Ancestral State Reconstructions, and Tests for Selection

Full-length PI^L coding sequence alignments were generated using MUSCLE, as implemented in Geneious, and refined by hand. Two matrices were generated: One that had all full-length PI-like sequence data for the monocots and select outgroups, and another that included only those sequences for which dimerization data existed. Sequences we generated have been deposited on GenBank KU740296-KU740323. Model and partitioning scheme selection was performed using PartitionFinder. Bayesian reconstruction of phylogeny was conducted using MrBayes v3.2.1. Maximum-likelihood reconstruction was conducted using RAxML, as implemented on the CIPRES server. Ancestral sequence reconstruction was performed using the DataMonkey webserver, and Lazarus. Ancestral dimerization states were reconstructed using both maximum likelihood and parsimony in Mesquite

v2.75. The tests for selection included branch-sites REL (Kosakovsky Pond et al. 2011), MEDS, fixed effects episodic diversifying selection (Murrell et al. 2012), and DEPS (Kosakovsky Pond et al. 2008) tests in Hyphy v2.2 (Pond et al. 2005) or using the DataMonkey webserver (Kosakovsky Pond and Frost 2005a), and the branch-sites test in PAML v4.8 (Yang 2007).

Domain Swaps and Site-Directed Mutagenesis

Chimeric *Joinvillea*-PI (J-PI), *Zea* PI-2 (STS1) proteins were constructed using overlap extension followed by high-fidelity polymerase chain reaction (PCR) (Warrens et al. 1997; Atanassov et al. 2009). All primers used are listed in supplementary table S3, Supplementary Material online. Initial PCR reactions contained 0.75 units of Taq polymerase (NEB), 10% dimethyl sulfoxide (DMSO), forward and reverse primers (0.5 μM each), dNTPs (0.25 mM each), $MgCl_2$ (1.7 mM), and 50 ng of template plasmid DNA in a 1× buffered solution. Individual amplified domains were gel extracted and purified using the Promega Wizard SV Gel Clean-Up system and quantified using a NanoDrop spectrophotometer (ThermoFisher) before overlap extension. Overlap extension reactions contained 0.6 units of Phusion polymerase (ThermoFisher), dNTPs (0.2 mM each), and template DNA (approximately 270 ng of PCR product for each domain). Following ten cycles of overlap extension (cycling conditions: 98 °C for 10 s, 60 °C for 30 s, 72 °C for 1 min for ten cycles), the polymerase was replenished and amplification primers added to a final concentration of 0.4 μM. Chimeric DNA fragments were amplified in a final touchdown PCR reaction. Resulting PCR products were cloned into pJET1.2 for Sanger sequencing and then subcloned into pSPUTK.

Site-directed mutagenesis was performed using the Quikchange II or the Quikchange II XL kits from Agilent using primers designed using Agilent's online primer design tool (supplementary table S3, Supplementary Material online; http://www.genomics.agilent.com/primerDesignProgram.jsp, last accessed March 3, 2015). Mutagenesis was conducted on 50 ng of plasmid DNA, for ten cycles, according to manufacturers' instructions. Correct clones were verified using PCR and Sanger sequencing.

Homology Modeling and Assessment of Sequence Conservation

The SWISS-MODEL server was used to search the protein databank for appropriate structural templates, generate pairwise alignments, and model B-class protein structure (Arnold et al. 2006; Biasini et al. 2014). B-class proteins from the Poales were modeled against protein databank templates (1egw and 3mu6) for comparative analyses (Berman et al. 2000; Santelli and Richmond 2000; Jayathilaka et al. 2012). A ConSurf analysis was conducted using an alignment of all available PI-like genes from the monocots (Landau et al. 2005).

Arabidopsis Transformations

cDNA sequences of *Joinvillea-PI* and *STS1*, both under the synthetic 10-Op promoter (Baroux et al. 2005), were cloned into pBJ36. The promoter-gene constructs were then subcloned into the Not1 site of the pMLBART27 binary vector. Clones were transferred into *Agrobacterium tumefasciens*, which was subsequently used to transform *A. thaliana Ler* containing the synthetic RNA polymerase Lhg4 under either the *AP1* or *AP3* promoter from *Arabidopsis*. The resulting *Arabidopsis* transformants were crossed to either the *ap3-4* (Jack et al. 1992) or *pi-1* (Goto and Meyerowitz 1994) mutants and F2–F5 progeny from these crosses were characterized.

Supplementary Material

Supplementary figures S1–S6 and tables S1–S3 are available at *Molecular Biology and Evolution* online (http://www.mbe.oxfordjournals.org/).

Acknowledgments

The authors are very grateful for those who provided them with samples, especially J. Travis Columbus and Simon Malcomber. They thank Mackenzie Barber, Ryan Desrochers, and Tiffany Ma for help with genotyping. They also thank Courtney Babbitt and two anonymous reviewers for valuable suggestions for improving an earlier version of the manuscript. This work was supported by a grant from the National Science Foundation (IOS-1025121 to C.J.W.).

References

Adhikary S, Eilers M. 2005. Transcriptional regulation and transformation by Myc proteins. *Nat Rev Mol Cell Biol*. 6:635–645.

Airoldi CA, Bergonzi S, Davies B. 2010. Single amino acid change alters the ability to specify male or female organ identity. *Proc Nat Acad Sci U S A*. 107:18898–18902.

Ambrose BA, Lerner DR, Ciceri P, Padilla CM, Yanofsky MF, Schmidt RJ. 2000. Molecular and genetic analyses of the *silky1* gene reveal conservation in floral organ specification between eudicots and monocots. *Mol Cell*. 5:569–579.

Arnold K, Bordoli L, Kopp J, Schwede T. 2006. The SWISS-MODEL workspace: a web-based environment for protein structure homology modelling. *Bioinformatics* 22:195–201.

Atanassov II, Atanassov II, Etchells JP, Turner SR. 2009. A simple, flexible and efficient PCR-fusion/Gateway cloning procedure for gene fusion, site-directed mutagenesis, short sequence insertion and domain deletions and swaps. *Plant Methods*. 5:14.

Baker CR, Booth LN, Sorrells TR, Johnson AD. 2012. Protein modularity, cooperative binding, and hybrid regulatory states underlie transcriptional network diversification. *Cell* 151:80–95.

Baroux C, Blanvillain R, Betts H, Batoko H, Craft J, Martinez A, Gallois P, Moore I. 2005. Predictable activation of tissue-specific expression from a single gene locus using the pOp/LhG4 transactivation system in Arabidopsis. *Plant Biotechnol J*. 3:91–101.

Bartlett ME, Whipple CJ. 2013. Protein change in plant evolution: tracing one thread connecting molecular and phenotypic diversity. *Front Plant Sci*. 4:382.

Bartlett ME, Williams SK, Taylor Z, DeBlasio S, Goldshmidt A, Hall DH, Schmidt RJ, Jackson DP, Whipple CJ. 2015. The Maize PI/GLO Ortholog Zmm16/sterile tassel silky ear1 interacts with the zygomorphy and sex determination pathways in flower development. *Plant Cell*. 27:3081–3098.

Berman HM, Westbrook J, Feng Z, Gilliland G, Bhat TN, Weissig H, Shindyalov IN, Bourne PE. 2000. The Protein Data Bank. *Nucleic Acids Res*. 28:235–242.

Biasini M, Bienert S, Waterhouse A, Arnold K, Studer G, Schmidt T, Kiefer F, Cassarino TG, Bertoni M, Bordoli L, et al. 2014. SWISS-MODEL: modelling protein tertiary and quaternary structure using evolutionary information. *Nucleic Acids Research* 42:W252–W258.

Bouchenak-Khelladi Y, Muasya AM, Linder HP. 2014. A revised evolutionary history of Poales: origins and diversification. *Bot J Linn Soc*. 175:4–16.

Brayer KJ, Lynch VJ, Wagner GP. 2011. Evolution of a derived protein-protein interaction between HoxA11 and Foxo1a in mammals caused by changes in intramolecular regulation. *Proc Nat Acad Sci U S A*. 108:E414–E420.

Carroll S. 2000. Endless forms: the evolution of gene regulation and morphological diversity. *Cell* 101:577.

Carroll SB. 2005. Evolution at two levels: on genes and form. *PLoS Biol*. 3:e245.

Chen M-K, Hsieh W-P, Yang C-H. 2011. Functional analysis reveals the possible role of the C-terminal sequences and PI motif in the function of lily (Lilium longiflorum) PISTILLATA (PI) orthologues. *J Exp Bot*. doi: 10.1093/jxb/err323.

Chia J-M, Song C, Bradbury PJ, Costich D, de Leon N, Doebley J, Elshire RJ, Gaut B, Geller L, Glaubitz JC. 2012. Maize HapMap2 identifies extant variation from a genome in flux. *Nat Genetics*. 44:803–807.

Coen ES, Meyerowitz EM. 1991. The war of the whorls: genetic interactions controlling flower development. *Nature* 353:31–37.

Cui H, Levesque MP, Vernoux T, Jung JW, Paquette AJ, Gallagher KL, Wang JY, Blilou I, Scheres B, Benfey PN. 2007. An evolutionarily conserved mechanism delimiting SHR movement defines a single layer of endodermis in plants. *Science* 316:421–425.

Culley TM, Weller SG, Sakai AK. 2002. The evolution of wind pollination in angiosperms. *Trends Ecol Evol*. 17:361–369.

Davies KA, Bergmann DC. 2014. Functional specialization of stomatal bHLHs through modification of DNA-binding and phosphoregulation potential. *Proc Nat Acad Sci U S A*. 111:15585–15590.

de Folter S, Immink RG, Kieffer M, Parenicova L, Henz SR, Weigel D, Busscher M, Kooiker M, Colombo L, Kater MM, et al. 2005. Comprehensive interaction map of the arabidopsis MADS Box transcription factors. *Plant Cell*. 17:1424–1433.

de Martino G, Pan I, Emmanuel E, Levy A, Irish VF. 2006. Functional analyses of two tomato APETALA3 genes demonstrate diversification in their roles in regulating floral development. *Plant Cell*. 18:1833–1845.

Della Pina S, Souer E, Koes R. 2014. Arguments in the evo-devo debate: say it with flowers!. *J Exp Bot*. 65:2231–2242.

Drea S, Hileman LC, de Martino G, Irish VF. 2007. Functional analyses of genetic pathways controlling petal specification in poppy. *Development* 134:4157–4166.

Fourquin C, del Cerro C, Victoria FC, Vialette-Guiraud A, de Oliveira AC, Ferrándiz C. 2013. A change in SHATTERPROOF protein lies at the origin of a fruit morphological novelty and a new strategy for seed dispersal in Medicago genus. *Plant Physiol*. 162:907–917.

Friedman J, Barrett SCH. 2008. A phylogenetic analysis of the evolution of wind pollination in the angiosperms. *Int J Plant Sci*. 169:49–58.

Furumizu C, Alvarez JP, Sakakibara K, Bowman JL. 2015. Antagonistic Roles for KNOX1 and KNOX2 genes in patterning the land plant body plan following an ancient gene duplication. *PLoS Genetics*. 11:e1004980-e1004980.

Galimba KD, Tolkin TR, Sullivan AM, Melzer R, Theissen G, Di Stilio VS. 2012. Loss of deeply conserved C-class floral homeotic gene function and C- and E-class protein interaction in a double-flowered ranunculid mutant. *Proc Nat Acad Sci U S A*. 109:E2267–E2275.

Gallavotti A, Malcomber S, Gaines C, Stanfield S, Whipple C, Kellogg E, Schmidt RJ. 2011. BARREN STALK FASTIGIATE1 is an AT-hook protein required for the formation of maize ears. *Plant Cell*. 23:1756–1771.

Geuten K, Irish V. 2010. Hidden variability of floral homeotic B genes in solanaceae provides a molecular basis for the evolution of novel functions. *Plant Cell*. 22:2562–2578.

Geuten K, Viaene T, Irish VF. 2011. Robustness and evolvability in the B-system of flower development. *Ann Bot*. 107:1545–1556.

Givnish TJ, Ames M, McNeal JR, McKain MR, Steele PR, dePamphilis CW, Graham SW, Pires JC, Stevenson DW, Zomlefer WB. 2010. Assembling the tree of the monocotyledons: plastome sequence phylogeny and evolution of Poales 1. *Ann Missouri Bot Gard*. 97:584–616.

Goto K, Meyerowitz EM. 1994. Function and regulation of the *Arabidopsis* floral homeotic gene *PISTILLATA*. *Genes Dev*. 8:1548–1560.

GPWG II GPWGI 2012. New grass phylogeny resolves deep evolutionary relationships and discovers C4 origins. *New Phytol*. 193:304–312.

Halfter U, Ali N, Stockhaus J, Ren L, Chua NH. 1994. Ectopic expression of a single homeotic gene, the Petunia gene green petal, is sufficient to convert sepals to petaloid organs. *Embo J*. 13:1443–1449.

Hernandez-Hernandez T, Martinez-Castilla LP, Alvarez-Buylla ER. 2007. Functional diversification of B MADS-Box homeotic regulators of flower development: adaptive evolution in protein-protein interaction domains after major gene duplication events. *Mol Biol Evol*. 24:465–481.

Hill TA, Day CD, Zondlo SC, Thackeray AG, Irish VF. 1998. Discrete spatial and temporal cis-acting elements regulate transcription of the Arabidopsis floral homeotic gene APETALA3. *Development* 125:1711–1721.

Hoekstra HE, Coyne JA. 2007. The locus of evolution: evo devo and the genetics of adaptation. *Evolution* 61:995–1016.

Honma T, Goto K. 2001. Complexes of MADS-box proteins are sufficient to convert leaves into floral organs. *Nature* 409:525–529.

Hughes AL, Nei M. 1988. Pattern of nucleotide substitution at major histocompatibility complex class I loci reveals overdominant selection. *Nature* 335:167–170.

Immink RG, Kaufmann K, Angenent GC. 2010. The "ABC" of MADS domain protein behaviour and interactions. *Semin Cell Dev Biol*. 21:87–93.

Jack T, Brockman LL, Meyerowitz EM. 1992. The homeotic gene *APETALA3* of *Arabidopsis thaliana* encodes a MADS box and is expressed in petals and stamens. *Cell* 68:683–697.

Jack T, Fox GL, Meyerowitz EM. 1994. Arabidopsis homeotic gene APETALA3 ectopic expression: transcriptional and posttranscriptional regulation determine floral organ identity. *Cell* 76:703–716.

Jayathilaka N, Han A, Gaffney KJ, Dey R, Jarusiewicz JA, Noridomi K, Philips MA, Lei X, He J, Ye J. 2012. Inhibition of the function of class IIa HDACs by blocking their interaction with MEF2. *Nucleic Acids Res*. 40:5378–5388.

Jetha K, Theißen G, Melzer R. 2014. Arabidopsis SEPALLATA proteins differ in cooperative DNA-binding during the formation of floral quartet-like complexes. *Nucleic Acids Res*. 42:10927–10942.

Kanaoka MM, Pillitteri LJ, Fujii H, Yoshida Y, Bogenschutz NL, Takabayashi J, Zhu J-K, Torii KU. 2008. SCREAM/ICE1 and SCREAM2 specify three cell-state transitional steps leading to Arabidopsis stomatal differentiation. *Plant Cell*. 20:1775–1785.

Kang H-G, Jeon J-S, Lee S, An G. 1998. Identification of class B and class C floral organ identity genes from rice plants. *Plant Mol Biol*. 38:1021–1029.

Kanno A, Saeki H, Kameya T, Saedler H, Theissen G. 2003. Heterotopic expression of class B floral homeotic genes supports a modified ABC model for tulip (*Tulipa gesneriana*). *Plant Mol Biol*. 52:831–841.

Kaufmann K, Melzer R, Theissen G. 2005. MIKC-type MADS-domain proteins: structural modularity, protein interactions and network evolution in land plants. *Gene* 347:183–198.

Kaufmann K, Muiño JM, Jauregui R, Airoldi CA, Smaczniak C, Krajewski P, Angenent GC. 2009. Target genes of the MADS transcription factor SEPALLATA3: integration of developmental and hormonal pathways in the *Arabidopsis* flower. *PLoS Biol*. 7:e1000090.

Kellogg EA. 2015. Flowering plants. Monocots: Poaceae. Berlin: Springer.

Kim ST, Yoo MJ, Albert VA, Farris JS, Soltis PS, Soltis DE. 2004. Phylogeny and diversification of B-function MADS-box genes in angiosperms: evolutionary and functional implications of a 260-million-year-old duplication. *Am J Bot*. 91:2102–2118.

Kong Q, Pattanaik S, Feller A, Werkman JR, Chai C, Wang Y, Grotewold E, Yuan L. 2012. Regulatory switch enforced by basic helix-loop-helix and ACT-domain mediated dimerizations of the maize transcription factor R. *Proc Nat Acad Sci U S A*. 109:E2091–E2097.

Kosakovsky Pond SL, Frost SDW. 2005a. DataMonkey: rapid detection of selective pressure on individual sites of codon alignments. *Bioinformatics* 21:2531–2533.

Kosakovsky Pond SL, Frost SDW. 2005b. Not so different after all: a comparison of methods for detecting amino acid sites under selection. *Mol Biol Evol*. 22:1208–1222.

Kosakovsky Pond SL, Murrell B, Fourment M, Frost SDW, Delport W, Scheffler K. 2011. A random effects branch-site model for detecting episodic diversifying selection. *Mol Biol Evol*. 28:3033–3043.

Kosakovsky Pond SL, Poon AFY, Leigh Brown AJ, Frost SDW. 2008. A maximum likelihood method for detecting directional evolution in protein sequences and its application to Influenza A virus. *Mol Biol Evol*. 25:1809–1824.

Kramer EM, Holappa L, Gould B, Jaramillo MA, Setnikov D, Santiago PM. 2007. Elaboration of B gene function to include the identity of novel floral organs in the lower eudicot *Aquilegia*. *Plant Cell*. 19:750–766.

Krizek BA, Meyerowitz EM. 1996a. The Arabidopsis homeotic gene *APETALA3* and *PISTILLATA* are sufficient to provide the B class organ identity function. *Development* 122:11–22.

Krizek BA, Meyerowitz EM. 1996b. Mapping the protein regions responsible for the functional specificities of the Arabidopsis MADS domain organ-identity proteins. *Proc Nat Acad Sci U S A*. 93:4063–4070.

Kyozuka J, Kobayashi T, Morita M, Shimamoto K. 2000. Spatially and temporally regulated expression of rice MADS box genes with similarity to Arabidopsis class A, B and C genes. *Plant Cell Physiol*. 41:710–718.

Lamb RS, Hill TA, Tan QKG, Irish VF. 2002. Regulation of APETALA3 floral homeotic gene expression by meristem identity genes. *Development* 129:2079–2086.

Landau M, Mayrose I, Rosenberg Y, Glaser F, Martz E, Pupko T, Ben-Tal N. 2005. ConSurf 2005: the projection of evolutionary conservation scores of residues on protein structures. *Nucleic Acids Res*. 33:W299–W302.

Lange M, Orashakova S, Lange S, Melzer R, Theissen G, Smyth DR, Becker A. 2013. The *seirena* B class floral homeotic mutant of California poppy (*Eschscholzia californica*) reveals a function of the Enigmatic PI motif in the formation of specific multimeric MADS domain protein complexes. *Plant Cell*. 25:438–53.

Lau OS, Davies KA, Chang J, Adrian J, Rowe MH, Ballenger CE, Bergmann DC. 2014. Direct roles of SPEECHLESS in the specification of stomatal self-renewing cells. *Science* 345:1605–1609.

Lenser T, Theissen G, Dittrich P. 2009. Developmental robustness by obligate interaction of class B floral homeotic genes and proteins. *PLoS Comput Biol*. 5:e1000264.

Leseberg CH, Eissler CL, Wang X, Johns MA, Duvall MR, Mao L. 2008. Interaction study of MADS-domain proteins in tomato. *J Exp Bot*. 59:2253–2265.

Linder H. 1998. Morphology and the evolution of wind pollination. Reproductive biology in systematics, conservation and economic botany. Kew (United Kingdom): Royal Botanic Garden. p. 123–135.

Litt A, Kramer EM. 2010. The ABC model and the diversification of floral organ identity. *Semin Cell Dev Biol*. 21:129–137.

Liu C, Zhang J, Zhang N, Shan H, Su K, Zhang J, Meng Z, Kong H, Chen Z. 2010. Interactions among proteins of floral MADS-box genes in basal Eudicots: implications for evolution of the regulatory network for flower development. *Mol Biol Evol*. 27:1598–1611.

Löhr U, Pick L. 2005. Cofactor-interaction motifs and the cooption of a homeotic Hox protein into the segmentation pathway of Drosophila melanogaster. *Curr Biol*. 15:643–649.

Lynch M, O'Hely M, Walsh B, Force A. 2001. The probability of preservation of a newly arisen gene duplicate. *Genetics* 159:1789–1804.

Lynch VJ, Tanzer A, Wang Y, Leung FC, Gellersen B, Emera D, Wagner GP. 2008. Adaptive changes in the transcription factor HoxA-11 are essential for the evolution of pregnancy in mammals. *Proc Nat Acad Sci U S A*. 105:14928–14933.

Lynch VJ, Wagner GP. 2008. Resurrecting the role of transcription factor change in developmental evolution. *Evolution* 62:2131–2154.

Maddison W, Maddison D. 2009. Mesquite: A modular system for evolutionary analysis. Version 2.72. Available from: http://mesquiteproject.org.

Mandel MA, Gustafson-Brown C, Savidge B, Yanofsky MF. 1992. Molecular characterization of the Arabidopsis floral homeotic gene *APETALA1*. *Nature* 360:273–277.

Melzer R, Härter A, Rümpler F, Kim S, Soltis PS, Soltis DE, Theißen G 2014. DEF-and GLO-like proteins may have lost most of their interaction partners during angiosperm evolution. *Ann Bot*. 114:1431–43.

Melzer R, Theißen G. 2009. Reconstitution of "floral quartets" in vitro involving class B and class E floral homeotic proteins. *Nucleic Acids Res*. 37:2723–2736.

Mendes MA, Guerra RF, Berns MC, Manzo C, Masiero S, Finzi L, Kater MM, Colombo L. 2013. MADS domain transcription factors mediate short-range DNA looping that is essential for target gene expression in Arabidopsis. *Plant Cell*. 25:2560–2572.

Mondragon-Palomino M, Hiese L, Haerter A, Koch MA, Theissen G. 2009. Positive selection and ancient duplications in the evolution of class B floral homeotic genes of orchids and grasses. *BMC Evol Biol*. 9:81.

Moon YH, Jung JY, Kang HG, An GH. 1999. Identification of a rice APETALA3 homologue by yeast two-hybrid screening. *Plant Mol Biol*. 40:167–177.

Munster T, Wingen LU, Faigl W, Werth S, Saedler H, Theissen G. 2001. Characterization of three *GLOBOSA*-like MADS-box genes from maize: evidence for ancient paralogy in one class of floral homeotic B-function genes of grasses. *Gene* 262:1–13.

Murrell B, de Oliveira T, Seebregts C, Kosakovsky Pond SL, Scheffler K, on behalf of the Southern African T, Resistance Network C. 2012. Modeling HIV-1 drug resistance as Episodic directional selection. *PLoS Comput Biol*. 8:e1002507.

Nagasawa N, Miyoshi M, Sano Y, Satoh H, Hirano H, Sakai H, Nagato Y. 2003. SUPERWOMAN1 and DROOPING LEAF genes control floral organ identity in rice. *Development* 130:705–718.

Ng M, Yanofsky MF. 2001. Activation of the Arabidopsis B class homeotic genes by APETALA1. *Plant Cell*. 13:739–753.

Ó'Maoiléidigh DS, Graciet E, Wellmer F. 2014. Gene networks controlling *Arabidopsis thaliana* flower development. *New Phytol*. 201:16–30.

Paaby AB, Rockman MV. 2014. Cryptic genetic variation: evolution's hidden substrate. *Nat Rev Genetics*. 15:247–258.

Pelaz S, Ditta G, Baumann E, Wisman E, Yanofsky M. 2000. B and C floral organ identity functions require *SEPALLATA* MADS-box genes. *Nature* 405:200–203.

Pellegrini L, Tan S, Richmond TJ. 1995. Structure of serum response factor core bound to DNA. *Nature* 376:490–498.

Pond SLK, Frost SDW, Muse SV. 2005. HyPhy: hypothesis testing using phylogenies. *Bioinformatics* 21:676–679.

Prasad K, Vijayraghavan U. 2003. Double-stranded RNA interference of a rice *PI/GLO* paralog, *OsMADS2*, uncovers its second-whorl-specific function in floral organ patterning. *Genetics* 165:2301–2305.

Puranik S, Acajjaoui S, Conn S, Costa L, Conn V, Vial A, Marcellin R, Melzer R, Brown E, Hart D. 2014. Structural basis for the oligomerization of the MADS domain transcription factor SEPALLATA3 in Arabidopsis. *Plant Cell*. 26:3603–3615.

Quinet M, Bataille G, Dobrev PI, Capel C, Gomez P, Capel J, Lutts S, Motyka V, Angosto T, Lozano R. 2014. Transcriptional and hormonal regulation of petal and stamen development by STAMENLESS, the tomato (*Solanum lycopersicum* L.) orthologue to the B-class APETALA3 gene. *J Exp Bot*. 65:2243–2256.

Renner T, Specht CD. 2012. Molecular and functional evolution of class I chitinases for plant carnivory in the Caryophyllales. *Mol Biol Evol*. 29:2971–85.

Riechmann JL, Krizek BA, Meyerowitz EM. 1996. Dimerization specificity of Arabidopsis MADS domain homeotic proteins APETALA1, APETALA3, PISTILLATA, and AGAMOUS. *Proc Nat Acad Sci U S A*. 93:4793–4798.

Riechmann JL, Wang M, Meyerowitz EM. 1996. DNA-binding properties of *Arabidopsis* MADS domain homeotic proteins APETALA1, APETALA3, PISTILLATA and AGAMOUS. *Nucleic Acids Res*. 24:3134–3141.

Ronai Z, Wang Y, Khandurina J, Budworth P, Sasvari-Szekely M, Wang X, Guttman A. 2003. Transcription factor binding study by capillary zone electrophoretic mobility shift assay. *Electrophoresis* 24:96–100.

Roque E, Serwatowska J, Cruz Rochina M, Wen J, Mysore KS, Yenush L, Beltran JP, Canas LA. 2013. Functional specialization of duplicated AP3-like genes in *Medicago truncatula*. *Plant J*. 73:663–675.

Sabatini S, Heidstra R, Wildwater M, Scheres B. 2003. SCARECROW is involved in positioning the stem cell niche in the Arabidopsis root meristem. *Genes Dev*. 17:354–358.
Santelli E, Richmond TJ. 2000. Crystal structure of MEF2A core bound to DNA at 1.5 Å resolution. *J Mol Biol*. 297:437–449.
Sayou C, Monniaux M, Nanao MH, Moyroud E, Brockington SF, Thévenon E, Chahtane H, Warthmann N, Melkonian M, Zhang Y. 2014. A promiscuous intermediate underlies the evolution of LEAFY DNA binding specificity. *Science* 343:645–648.
Schmid M, Davison TS, Henz SR, Pape UJ, Demar M, Vingron M, Scholkopf B, Weigel D, Lohmann JU. 2005. A gene expression map of *Arabidopsis thaliana* development. *Nat Genetics*. 37:501–506.
Schwarz-Sommer Z, Hue I, Huijser P, Flor PJ, Hansen R, Tetens F, Loennig WE, Saedler H, Sommer H. 1992. Characterization of the Antirrhinum floral homeotic mads-box gene deficiens evidence for DNA binding and autoregulation of its persistent expression throughout flower development. *EMBO J*. 11:251–264.
Sharma B, Kramer E. 2013. Sub- and neo-functionalization of APETALA3 paralogs have contributed to the evolution of novel floral organ identity in Aquilegia (columbine, Ranunculaceae). *New Phytol* 197:949–957.
Singh R, Low E-TL, Ooi LC-L, Ong-Abdullah M, Ting N-C, Nagappan J, Nookiah R, Amiruddin MD, Rosli R, Manaf MAA, et al. 2013. The oil palm SHELL gene controls oil yield and encodes a homologue of SEEDSTICK. *Nature* 500:340–344.
Slattery M, Riley T, Liu P, Abe N, Gomez-Alcala P, Dror I, Zhou T, Rohs R, Honig B, Bussemaker HJ. 2011. Cofactor binding evokes latent differences in DNA binding specificity between Hox proteins. *Cell* 147:1270–1282.
Smaczniak C, Immink RG, Angenent GC, Kaufmann K. 2012. Developmental and evolutionary diversity of plant MADS-domain factors: insights from recent studies. *Development* 139:3081–3098.
Smaczniak C, Immink RG, Muino JM, Blanvillain R, Busscher M, Busscher-Lange J, Dinh QD, Liu S, Westphal AH, Boeren S, et al. 2012. Characterization of MADS-domain transcription factor complexes in Arabidopsis flower development. *Proc Natl Acad Sci U S A*. 109:1560–1565.
Sommer RJ. 2012. Evolution of regulatory networks: nematode vulva induction as an example of developmental systems drift. In: Soyer OS, editor. Evolutionary Systems Biology. Berlin: Springer. p. 79–91.
Specht CD, Bartlett ME. 2009. Flower Evolution: the origin and subsequent diversification of the Angiosperm flower. *Ann Rev Ecol Evol Syst*. 40:217–243.
Stern DL. 2000. Perspective: evolutionary developmental biology and the problem of variation. *Evolution* 54:1079–1091.
Stern DL, Orgogozo V. 2008. The loci of evolution: how predictable is genetic evolution? *Evolution* 62:2155–2177.
Tan S, Richmond TJ. 1998. Crystal structure of the yeast MATα2/MCM1/DNA ternary complex. *Nature* 391:660–666.
Theissen G, Melzer R. 2007. Molecular mechanisms underlying origin and diversification of the angiosperm flower. *Ann Bot*. 100:603–619.
Theissen G, Saedler H. 2001. Plant biology. Floral quartets. *Nature* 409:469–471.
True JR, Haag ES. 2001. Developmental system drift and flexibility in evolutionary trajectories. *Evol Dev*. 3:109–119.
Tsai W-C, Pan Z-J, Hsiao Y-Y, Jeng M-F, Wu T-F, Chen W-H, Chen H-H. 2008. Interactions of B-class complex proteins involved in tepal development in Phalaenopsis orchid. *Plant Cell Physiol*. 49:814–824.
Tuch BB, Li H, Johnson AD. 2008. Evolution of Eukaryotic transcription circuits. *Science* 319:1797–1799.
van Dijk ADJ, Morabito G, Fiers M, van Ham RCHJ, Angenent GC, Immink RGH. 2010. Sequence motifs in MADS transcription factors responsible for specificity and diversification of protein-protein interaction. *PLoS Comput Biol*. 6:e1001017.
Vandenbussche M, Zethof J, Royaert S, Weterings K, Gerats T. 2004. The duplicated B-class heterodimer model: whorl-specific effects and complex genetic interactions in *Petunia hybrida* flower development. *Plant Cell*. 16:741–754.
Veron AS, Kaufmann K, Bornberg-Bauer E. 2007. Evidence of interaction network evolution by whole-genome duplications: A case study in MADS-box proteins. *Mol Biol Evol*. 24:670–678.
Wagner A. 2005. Robustness and evolvability in living systems. Princeton (NJ): Princeton University Press.
Wagner A. 2011. The origins of evolutionary innovations: a theory of transformative change in living systems. Oxford University Press.
Warrens AN, Jones MD, Lechler RI. 1997. Splicing by overlap extension by PCR using asymmetric amplification: an improved technique for the generation of hybrid proteins of immunological interest. *Gene* 186:29–35.
Wei RX, Ge S. 2011. Evolutionary history and complementary selective relaxation of the duplicated PI genes in grasses. *J Integr Plant Biol*. 53:682–693.
Whipple CJ, Ciceri P, Padilla CM, Ambrose BA, Bandong SL, Schmidt RJ. 2004. Conservation of B-class floral homeotic gene function between maize and *Arabidopsis*. *Development* 131:6083–6091.
Whipple CJ, Schmidt RJ. 2006. Genetics of grass flower development. In: DE Soltis, JH Leebens-Mack, PS Soltis, JA Callow, editors. Advances in botanical research. Cambridge (MA): Academic Press. p. 385–424.
Whipple CJ, Zanis MJ, Kellogg EA, Schmidt RJ. 2007. Conservation of B class gene expression in the second whorl of a basal grass and outgroups links the origin of lodicules and petals. *Proc Natl Acad Sci U S A*.104:1081–1086.
Winter K-U, Weiser C, Kaufmann K, Bohne A, Kirchner C, Kanno A, Saedler H, Theissen G. 2002. Evolution of class B floral homeotic proteins: Obligate heterodimerization originated from homodimerization. *Mol Biol Evol*. 19:587–596.
Wittkopp PJ, Kalay G. 2012. Cis-regulatory elements: molecular mechanisms and evolutionary processes underlying divergence. *Nat Rev Genetics*. 13:59–69.
Wray GA, Hahn MW, Abouheif E, Balhoff JP, Pizer M, Rockman MV, Romano LA. 2003. The evolution of transcriptional regulation in eukaryotes. *Mol Biol Evol* 20:1377–1419.
Yadav SR, Prasad K, Vijayraghavan U. 2007. Divergent regulatory *OsMADS2* functions control size, shape and differentiation of the highly derived rice floret second-whorl organ. *Genetics* 176:283–294.
Yang Z, Bielawski JP. 2000. Statistical methods for detecting molecular adaptation. *Trends Ecol Evol*. 15:496–503.
Yang Y, Fanning L, Jack T. 2003. The K domain mediates heterodimerization of the Arabidopsis floral organ identity proteins, APETALA3 and PISTILLATA. *Plant J*. 33:47–59.
Yang Y, Jack T. 2004. Defining subdomains of the K domain important for protein-protein interactions of plant MADS proteins. *Plant Mol Biol*. 55:45–59.
Yang Y, Xiang H, Jack T. 2003. pistillata-5, an Arabidopsis B class mutant with strong defects in petal but not in stamen development. *Plant J*. 33:177–188.
Yang Z. 2007. PAML 4: phylogenetic analysis by maximum likelihood. *Mol Biol Evol*. 24:1586–1591.
Yao S-G, Ohmori S, Kimizu M, Yoshida H. 2008. Unequal genetic redundancy of rice *PISTILLATA* orthologs, *OsMADS2* and *OsMADS4*, in lodicule and stamen development. *Plant Cell Physiol*. 49:853–857.
Yasumura Y, Crumpton-Taylor M, Fuentes S, Harberd NP. 2007. Step-by-step acquisition of the gibberellin-DELLA growth-regulatory mechanism during land-plant evolution. *Curr Biol*. 17:1225–1230.
Zhang J, Nielsen R, Yang Z. 2005. Evaluation of an improved branch-site likelihood method for detecting positive selection at the molecular level. *Mol Biol Evol*. 22:2472–2479.
Zhang J-S, Li Z, Zhao J, Zhang S, Quan H, Zhao M, He C. 2014. Deciphering the *Physalis floridana* double-layered-lantern1 mutant provides insights into functional divergence of the GLOBOSA duplicates within the *Solanaceae*. *Plant Physiol*. 164:748–764.